Clim Dyn (2015) 44:1381–1401
DOI 10.1007/s00382-014-2126-4

The impact of westerly wind bursts and ocean initial state on the development, and diversity of El Niño events

Alexey V. Fedorov · Shineng Hu · Matthieu Lengaigne · Eric Guilyardi

Received: 16 October 2013 / Accepted: 18 March 2014 / Published online: 1 April 2014

Abstract Westerly wind bursts (WWBs) that occur in the western tropical Pacific are believed to play an important role in the development of El Niño events. Here, following the study of Lengaigne et al. (Clim Dyn 23(6):601–620, 2004), we conduct numerical simulations in which we reexamine the response of the climate system to an observed wind burst added to a coupled general circulation model. Two sets of twin ensemble experiments are conducted (each set has control and perturbed experiments). In the first set, the initial ocean heat content of the system is higher than the model climatology (recharged), while in the second set it is nearly normal (neutral). For the recharged state, in the absence of WWBs, a moderate El Niño with a maximum warming in the central Pacific (CP) develops in about a year. In contrast, for the neutral state, there develops a weak La Niña. However, when the WWB is imposed, the situation dramatically changes: the recharged state slides into an El Niño with a maximum warming in the eastern Pacific, while the neutral set produces a weak CP El Niño instead of previous La Niña conditions. The different response of the system to the exact same perturbations is controlled by the initial state of the ocean and the subsequent ocean–atmosphere interactions involving the interplay between the eastward shift of the warm pool and the warming of the eastern equatorial Pacific. Consequently, the observed diversity of El Niño, including the occurrence of extreme events, may depend on stochastic atmospheric processes, modulating El Niño properties within a broad continuum.

Keywords El Niño dynamics · El Niño flavors · Westerly wind bursts (WWB) · Climate models

A. V. Fedorov (✉) · S. Hu
Department of Geology and Geophysics, Yale University, New Haven, CT 06511, USA
e-mail: alexey.fedorov@yale.edu

M. Lengaigne · E. Guilyardi
IPSL/LOCEAN, Sorbonne Universités (UPMC-Paris 6, CNRS, IRD, MNHN), Paris, France

E. Guilyardi
NCAS Climate, Meteorology Department, University of Reading, Reading RG6 6BB, UK

1 Introduction

The El Niño-Southern Oscillation (ENSO) dominates climate variability in the tropical Pacific on interannual timescales and has far-reaching effects on climate (Philander 1990; Clarke 2008; Sarachik and Cane 2010). Although each El Niño event is unique (Fig. 1), from a theoretical perspective they all represent the warm phase of a natural mode of oscillations resulting from tropical ocean–atmosphere interactions (Jin and Neelin 1993a; Neelin and Jin 1993; Jin and Neelin 1993b; An and Jin 2001; Fedorov 2010). Various theories have been proposed to explain this mode with the delayed (Schopf and Suarez 1988; Battisti and Hirst 1989) and recharge-discharge oscillators (Jin 1997a, b) being most frequently cited; for generalization or extensions of these models see Fedorov (2010), Clarke (2010), Wang (2001), and others. Many studies suggest that in realistic regimes this internal mode is damped or neutrally-stable and stochastic atmospheric forcing is necessary to sustain a continual, albeit irregular oscillation (Fedorov and Philander 2000, 2001; Kessler 2002; Thompson and Battisti 2000, 2001; Philander and Fedorov 2003). Specifically, it has been argued that westerly wind bursts (WWBs) that sporadically occur in the western tropical Pacific may play an important role in ENSO dynamics (Fedorov 2002; Fedorov et al. 2003;

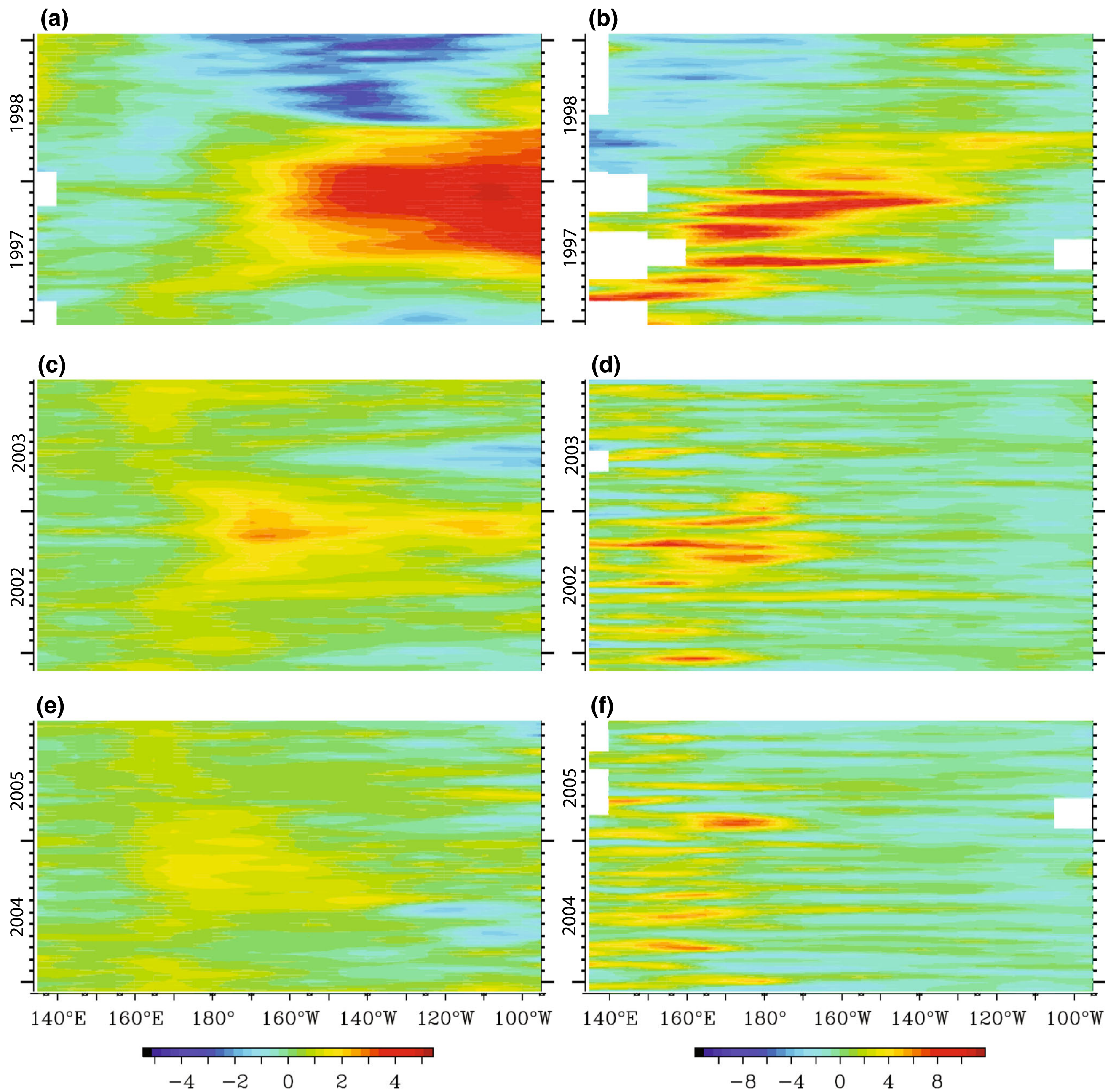

Fig. 1 Hovmoller diagrams of the observed SST anomalies (*left panels*; in °C) and zonal wind anomalies (*right panels*; in m/s) showing warm events of 1997/1998, 2002/2003, and 2004/2005. Note the huge differences between the events—from the strongest on the record El Niño of 1997–1998 to a warm episode of 2004 that reached about 2 °C in the central Pacific but mere 1 °C in the east. Data from the TAO project (http://www.pmel.noaa.gov/tao)

Lengaigne et al. 2004; Gebbie et al. 2007; Lopez et al. 2013) and might even trigger El Niño events on some occasions (Wyrtki 1975; McPhaden 1999; McPhaden and Yu 1999).

The present study focuses on the role that WWBs may play in the development of El Niño, and in particular, their contribution to the diversity of El Niño events. Observational and modeling studies suggest that WWBs can have a strong effect on some El Niño events. For example, a succession of WWBs preceding the 1997/1998 El Niño may have been responsible for the unusually large amplitude of that event (Boulanger and Menkes 1999; McPhaden 1999; McPhaden and Yu 1999; Boulanger et al. 2004). However, on other occasions WWBs have visibly little impact on the Niño3 index (Fedorov 2002; Shi et al. 2011). Why the response of the coupled system to WWBs differs so much from one occasion to the next remains an important question of tropical dynamics.

Models of various complexities have been used to understand the dynamical processes that control the impacts of WWBs. Using a simple coupled tropical ocean–atmosphere model, Fedorov (2002) argued that WWBs can affect El Niño, but the particular response of the coupled system depends on the mean state of the system and the timing of the burst with respect to the ENSO cycle. Other studies show that a WWB can push the warm pool edge eastward, promoting the occurrence of the subsequent bursts and shifting atmospheric convection eastward, which favors the development of El Niño events (Lengaigne et al. 2002, 2003; Eisenman et al. 2005; Vecchi et al. 2006; Drushka et al. 2014). Lengaigne et al. (2004) employ a comprehensive coupled GCM to demonstrate this strong positive feedback loop, and show that when the initial ocean heat content (OHC) is in the recharged state, a single intense WWB can increase the chance of El Niño events, via the Kelvin wave propagation, warm pool displacement, and resultant ocean–atmosphere interactions.

Recently, attention of many studies turned to the issue of the diversity of El Niño events, for instance in terms of the differences in the location of the maxima of sea surface temperature (SST) anomalies in the tropical Pacific (Larkin and Harrison 2005; Yu and Kao 2007; Ashok et al. 2007; Kao and Yu 2009; Yeh et al. 2009; Kug et al. 2009). These studies distinguish between the more conventional El Niño events with the maximum SST anomaly occurring in the eastern equatorial Pacific and those with the maximum in the central Pacific, typically referred to as Eastern Pacific (EP) El Niño and Central Pacific (CP) El Niño, respectively. Other terminologies have been also used, such as Cold Tongue El Niño and Warm Pool El Niño, or canonical El Niño and El Niño Modoki. It has been suggested that CP El Niño events may have been occurring more frequently during the last several decades (Ashok et al. 2007; Kao and Yu 2009; Kug et al. 2009; Lee and McPhaden 2010; Yeh et al. 2009) and that different flavors of El Niño may have different global climate impacts (Yu and Kim 2011; Hu et al. 2012; Zubiaurre and Calvo 2012; Kim et al. 2009; Gierach et al. 2012; Ding et al. 2011).

There is currently a debate on whether the two flavors of El Niño represent different types dynamically, or rather they are a part of a continuum of El Niño events. Kao and Yu (2009) argue that only local SST-atmosphere interactions are involved in the CP type, whereas Kug et al. (2009) emphasize the role of the zonal-advection feedback in the development of CP events. However, Ashok et al. (2007) show that thermocline variations induced by wind stress anomaly are as important to the development of CP El Niño. A related issue is how the different types are related to the SST and thermocline modes (Jin and Neelin 1993a, b; Fedorov and Philander 2001; Trenberth and Stepaniak 2001; Guilyardi 2006) and the previous classification exercises (Rasmusson and Carpenter 1982; Fedorov and Philander 2000; Kumar et al. 2006).

Several studies even dispute the reality of the statistical distinction between EP and CP Events, or the increasing occurrence of the latter during past decades, either arguing that the reliable record is too short to detect such a distinction (Nicholls 2008; McPhaden et al. 2011), or finding no distinction or trend using other statistical approaches (Giese and Ray 2011; Newman et al. 2011; Yeh et al. 2011; Lian and Chen 2012; L'Heureux et al. 2013). Some suggested that other classifications, such as standard versus extreme El Niño, could be more relevant (Lengaigne and Vecchi 2010; Takahashi et al. 2011).

Nevertheless, it is clear that El Niño does exhibit a strong diversity from one event to the next (Fig. 1). Consequently, since WWBs are shown to modulate the ENSO cycle, the question arises whether the activity of WWBs can affect the development and characteristics of El Niño events, resulting in the observed diversity. We will follow the approach of Lengaigne et al. (2004), in which a WWB taken from observations was superimposed in a suite of ensemble numerical experiments, but extend their approach to different initial ocean mean states and pay special attention to differences between CP and EP warming events. We will also investigate whether the thermocline feedback is important to both types of El Niño, and under which conditions extreme warm events, akin of El Niño of 1997/1998, can develop.

Thus, the aim of our study is to investigate the relationship between WWBs and El Niño characteristics within a comprehensive coupled GCM. Hereafter, to distinguish different flavors of El Niño, we will still use the CP and EP designations, since they do not *a priory* imply any physical mechanisms, but simply point to the geographical location of the maxima in SST anomalies. As our analysis will show, the dynamics of the two types of El Niño in our model are rather similar, but differ by the relative magnitude and details of the spatial structure of the driving terms.

This paper is organized as follows. Section 2 gives a brief introduction to the coupled model used in our study and the experimental approach. The results from two sets of experiments are discussed separately in Sect. 3, and then compared in Sect. 4. In Sect. 5, we discuss the heat budget analysis of the mixed layer temperature, concentrating on the role of the thermocline feedback in the development of warm events. In Sect. 6 we consider implications of this study for extreme El Niño events. The final section includes a summary and a brief discussion.

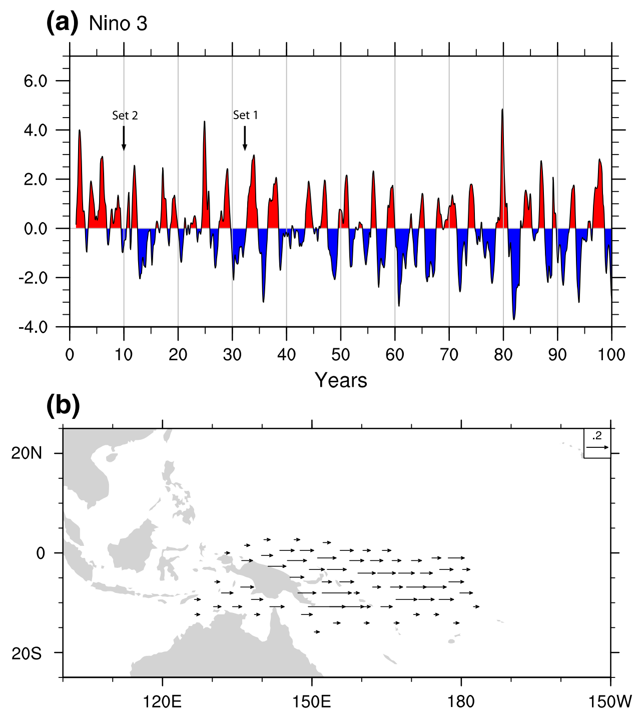

Fig. 2 **a** Interannual variations in the Niño3 index (°C) for the last 100 years of the model spin-up. **b** The spatial structure of the imposed westerly wind burst at its *peak*. The reference vector indicates 0.2 N/m^2. Note that the burst has a stronger signature in the Southern Hemisphere

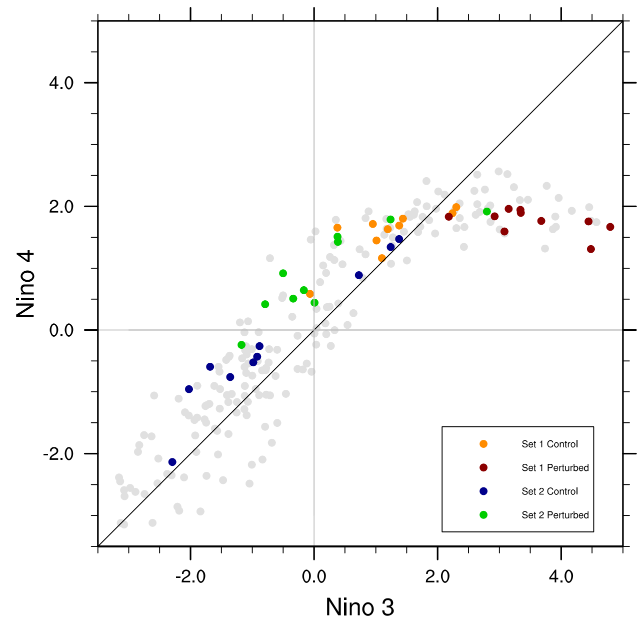

Fig. 3 A diagram showing the Niño4 index versus the Niño3 index (in °C) at the end of each year of the 200-year control run (*gray dots*). *Color dots* indicate the control and perturbed experiments to be discussed in detail in Sect. 7 (*cf.* Fig. 8a). Note the broad continuum of CP and EP El Niño events (*dots* in the upper half-plane above and below the diagonal, respectively). The Niño indices are averaged from October through December

2 The model and experimental set-up

2.1 The model

As in Lengaigne et al. (2004), we use a comprehensive climate GCM, HadOPA, which couples the OPA ocean model and the HadAM3 atmospheric model (http://www.met.reading.ac.uk/~ericg/Projects/hadopa_project.html). The OPA uses the global configuration ORCA. The horizontal resolution is 2° by 2° globally with a refinement to 0.5° in the meridional direction towards the equator. Vertically, there are 31 levels with the highest resolution (10 m) in the upper 150 m, and lowest resolution (500 m) in the deep ocean. For the HadAM3 atmosphere model, the horizontal resolution is 3.75° in longitude and 2.5° in latitude. There are 19 vertical levels with higher resolution in the boundary layer and around the tropopause. Through OASIS 2.4, the ocean and atmospheric GCMs are coupled via the air-sea fluxes and SST exchange everyday.

HadOPA is shown to represent well the tropical mean state, the seasonal cycle, and interannual variability. The model simulates a robust ENSO with a 3–4 year periodicity (Fig. 2a), having a broad continuum (Fig. 3) of EP and CP events to be discussed in the next sections. Roughly 1/3 of the events are of the EP type, and a similar fraction is of the CP type. The rest can be considered as mixed events (dots falling close to the diagonal in Fig. 3).

The two known shortcomings of the model, when compared to the observations, include a greater by 1 °C mean east–west SST gradient along the equator and a somewhat stronger variance of the Niño3 index (by approximately 30 % during the last 100 years of the control run). These issues are due to the relatively strong sensitivity of zonal winds to SST anomalies in the model. More details of the model description and validation can be found in Lengaigne et al. (2004, 2006), and references therein.

2.2 Numerical experiments

The coupled model is span up for 200 years. The last 100 years, when the system has nearly reached a statistical equilibrium, are used to compute the model climatology. Two sets of ensemble experiments are conducted, with the initial conditions picked from these 100 years (Fig. 2a). In Set 1, the initial ocean heat content of the system is recharged (OHC is higher than normal by about one standard deviation), while in Set 2 it is neutral (OHC anomaly with respect to the model climatology is near zero). Therefore, we will refer to Sets 1 and 2 as the recharged and neutral experiments, respectively.

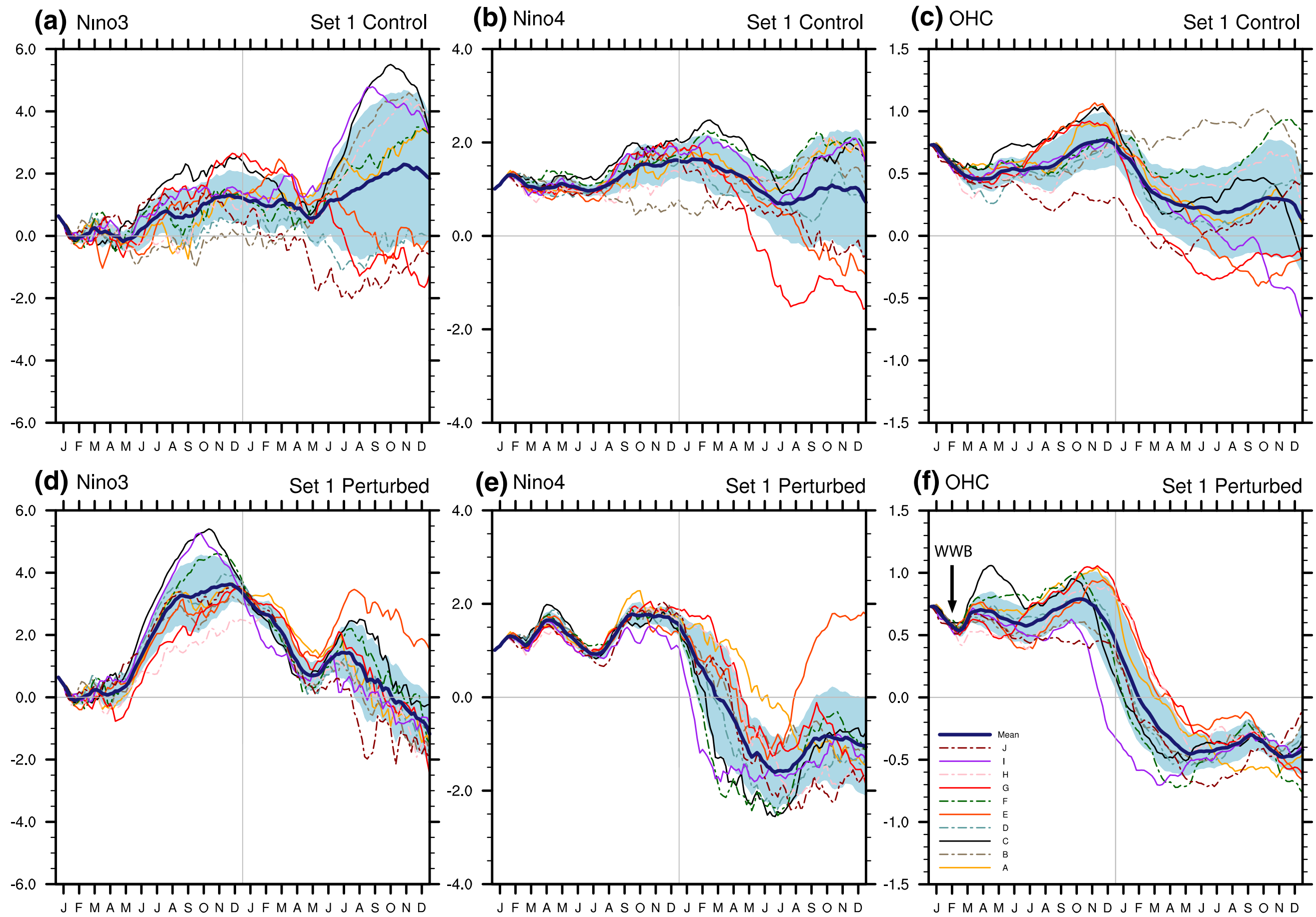

Fig. 4 Variations in the Niño3 and Niño4 indices (in °C) and anomalous OHC (in °C) for the control (*top row*) and perturbed (*bottom row*) experiments in Set 1 (recharged). For the perturbed experiments a WWB is imposed in mid-February. The Niño3 and Niño4 indices are defined as SST anomalies averaged in the regions 5°S–5°N, 150°W–90°W and 5°S–5°N, 160°E–150°W, respectively. The OHC anomaly is defined as temperature anomaly averaged from the ocean surface to a 300 m depth, between 5°S–5°N and 120°E–70°W. Thin color lines show ensemble members. *Thick blue lines* show ensemble means; *shading* indicates the corresponding standard deviation interval. Anomalies are computed with respect to the model climatology

Within each set, there are ten pairs of (control and perturbed) ensemble members, which share the same initial ocean state but have slightly different initial atmosphere conditions taken from ten successive model days. The perturbed experiments start with the same initial conditions as in the control experiments but include a superimposed westerly wind anomaly (Fig. 2b) added to the wind stress produced by the model itself in the tropical Pacific. Each experiment lasts 2 years.

As in Lengaigne et al. (2004), the superimposed westerly wind anomaly (the same in all perturbed experiments) corresponds to the westerly wind bursts observed in February–March 1997, prior to the strong El Niño event of that year. This WWB is imposed in mid-February and lasts for about 1 month. Figure 2b shows the imposed WWB at its peak, extending meridionally from 5°N to 15°S and zonally as far as to dateline. Figures 4f and 5f indicate that when the WWB is imposed in mid-February, the initial heat content of the system is recharged in Set 1 and neutral in Set 2. The larger OHC in Set 1 is associated with a stronger subsurface warming in the west, a greater extent of the Western Pacific warm pool, and a weaker cold tongue in the east (Fig. 6a–d).

3 Results

3.1 Experiments results: Set 1 (recharged)

Without the imposed WWBs, the ocean–atmosphere system in Set 1 slides into a CP El Niño event by the end of the first year as evident in the ensemble mean. During the first year, both the Niño3 and Niño4 indices increase gradually, but at the peak of the warm event the Niño4 index exceeds the Niño3 index by about 0.5 °C (Fig. 4a,b). The maximum of the SST anomaly during the warming is

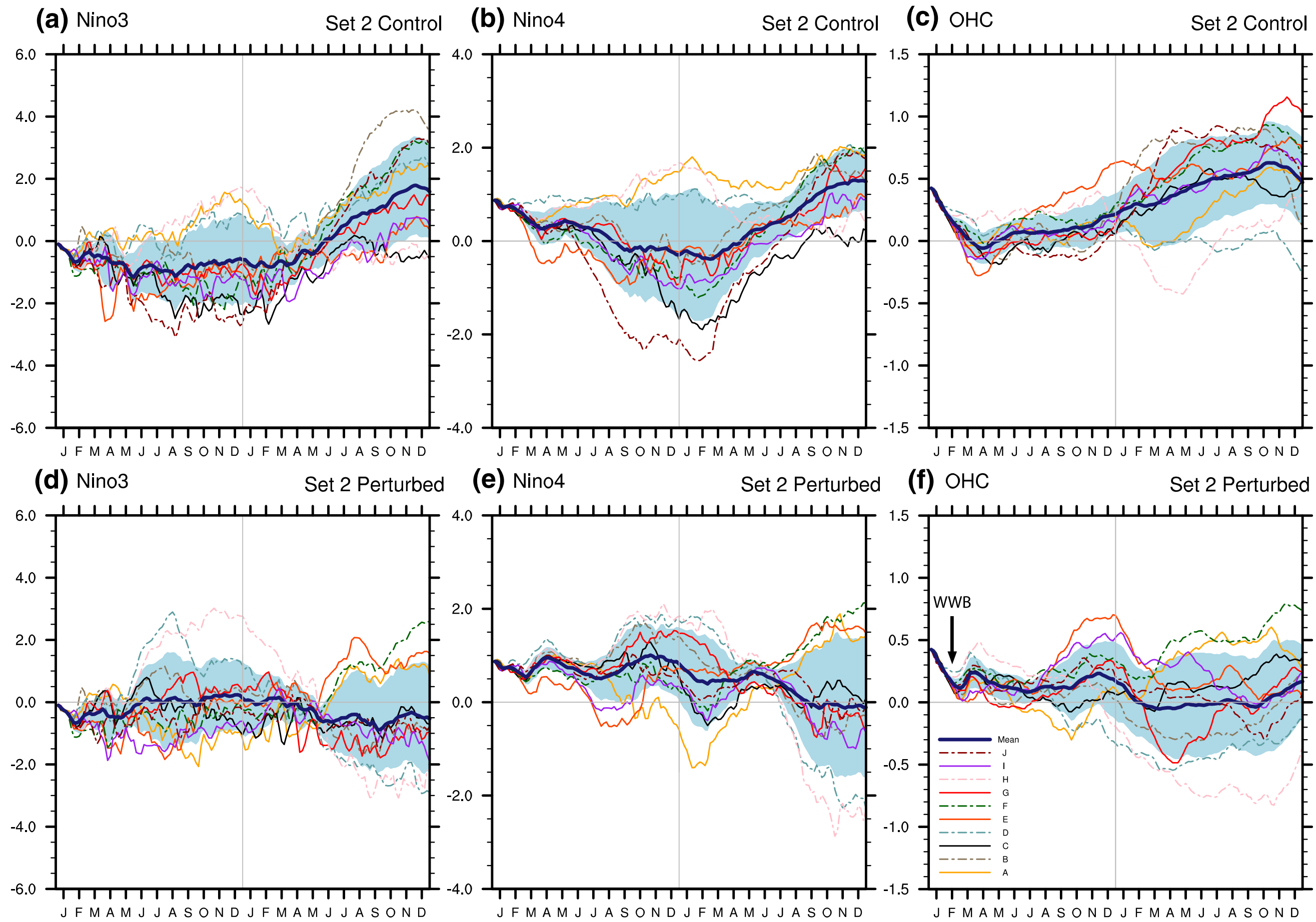

Fig. 5 As in Fig. 4 but for Set 2 (neutral)

located at about 170°W in the central Pacific region (Fig. 7a, c). Almost all of the ensemble members in Set 1 evolve into CP El Niño events, although the amplitude and location of the SST anomalies, and the relative magnitudes of the Niño3 and Niño4 indices, differ from one experiment to the next (Figs. 7a, 8).

The development of a CP El Niño in Set 1 Control is especially apparent in the Hovmoller diagrams showing the evolution of anomalies in SST, zonal wind stress, and surface zonal currents in the equatorial Pacific (Fig. 9a–c). During the early months of the first year, the ocean is in the recharged state and SST is higher than the climatology in most of the equatorial basin (Fig. 9a). Around April and May the model itself generates a relatively weak westerly wind anomaly (Fig. 9b) induced by the anomalous eastward extension of the eastern edge of the warm pool (Fig. 9a). This wind anomaly pushes the warm pool eastward locally via anomalous eastward currents (Fig. 9c) and induces SST anomalies in the central equatorial Pacific by generating a weak downwelling Kelvin wave, evident in zonal current (Fig. 9c) and thermocline anomalies (not shown), but those SST anomalies are small in the eastern Pacific. In fact, the eastern equatorial Pacific, east of 110°W, remains colder than the climatology until October. As a result, a CP El Niño develops with a local coupling between SST, winds, zonal currents (Fig. 9a–c) and thermocline mostly in the central Pacific.

During the second year, the coupled system transits from the CP El Niño event to a moderate EP El Niño due to subsequent ocean–atmosphere interactions; such a delayed evolution of El Niño into the next year was referred to as the “prolonged decaying pattern” by Yu and Kim (2010).

When a strong WWB is imposed in February–March (Fig. 2b), the situation changes dramatically: Set 1 develops into a strong EP El Niño, which reaches the maximum by November of the first year but lasts approximately 1½ years overall. The Niño3 index keeps increasing after the WWB is imposed, reaching 3.5 °C at the end of the first year (Fig. 4d), much higher than the Niño4 index (Fig. 4e). This is a typical EP El Niño event with the maximum of the SST anomaly located at ~130°W in the eastern equatorial Pacific during the warmest interval (Fig. 7e, g). After the impact of the imposed WWB, OHC shows much larger

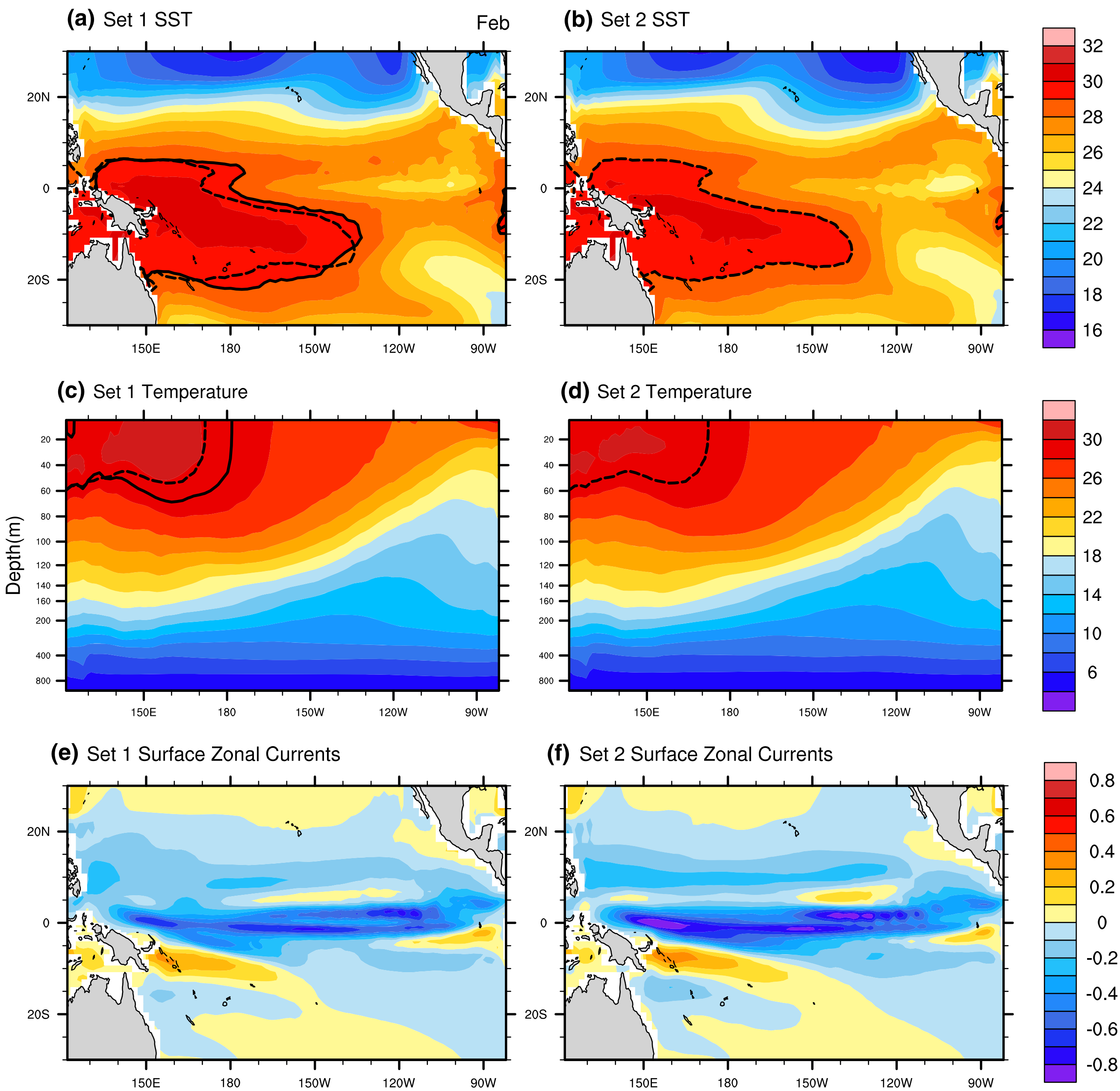

Fig. 6 The model initial state in February, when the WWB is applied, for Set 1 (*left*) and 2 (*right*) (in the ensemble-mean sense). From *top* to *bottom*: SST (in °C), temperature as a function of depth along the equator (in °C), and surface zonal currents (in m/s) are shown. The *solid* and *dashed lines* indicate the 29 °C isotherm for Set 1 and 2, respectively. Note the greater extent of the warm pool, a slightly warmer cold tongue, and weaker westward currents in Set 1

temporal variations, specifically a greater heat discharge after the warm event (Fig. 4f) characteristic of EP El Niño.

As expected, with the imposed WWB, the evolution of SST, zonal wind stress, and surface zonal currents also changes significantly as compared to the control runs. The imposed WWB affects the equatorial SST in two ways (local and remote). Firstly, the WWB pushes the warm pool eastward, warming the central Pacific (Fig. 9d); the coupling between the winds and SST facilitates the eastward shift of the warm pool together with wind stress anomalies. At the same time, the WWB induces a remote warming in the eastern equatorial Pacific about three months after the WWB (Fig. 9d), via a strong downwelling Kelvin wave (Fig. 9f). The initial warming in the central and eastern Pacific, due to both effects, generates strong westerly wind anomalies that propagate to the central Pacific (Fig. 9e), which relaxes the westward current and allows more SST warming (Fig. 9d, f) in via the positive

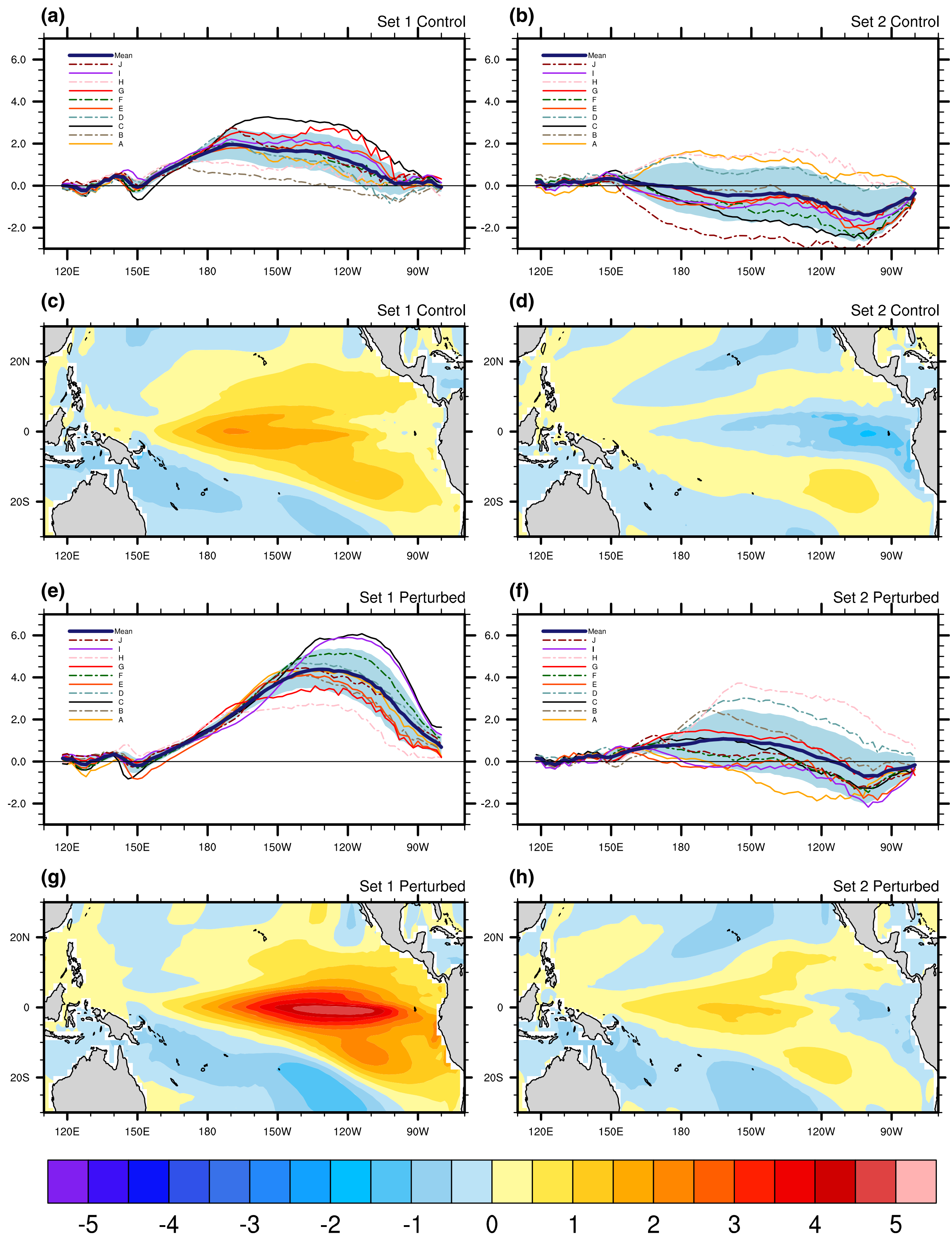
(a)
Set 1 Control
(b)
Set 2 Control
Mean
J
I
H
G
F
E
D
C
B
A
6.0
4.0
2.0
0.0
-2.0
120E
150E
180
150W
120W
90W
(c)
Set 1 Control
(d)
Set 2 Control
20N
0
20S
(e)
Set 1 Perturbed
(f)
Set 2 Perturbed
(g)
Set 1 Perturbed
(h)
Set 2 Perturbed
-5
-4
-3
-2
-1
0
1
2
3
4
5

◀**Fig. 7** Zonal and spatial structures of SST anomalies (in °C) near the peak of warm events for (**a**, **c**) Set 1 Control, (**b**, **d**) Set 2 Control, (**e**, **g**) Set 1 Perturbed, and (**f**, **h**) Set 2 Perturbed. *Thin color lines* show ensemble members. *Thick blue lines* show ensemble means; *shading* indicates the corresponding standard deviation interval. Contours intervals for SST anomalies are 0.5 °C. Anomalies are averaged from July to December and computed with respect to the model climatology

Bjerknes feedback (Lengaigne et al. 2003, 2004). The eastern equatorial Pacific, east of 110°W, becomes warmer than the climatology already in May, half-a-year earlier than in the control experiments. This allows an EP El Niño to develop further and reach a mature phase in the later months of the first year.

All the ensemble members evolve into EP El Niño events of varying magnitudes (Fig. 7e). The indices of SST and OHC diverge relatively little between the experiments especially within 1 year after the imposed perturbation (Fig. 4d–f). The shift from a CP El Niño to an EP El Niño after the WWB and the relatively moderate spread of ensemble members are apparent in the summary diagram of Fig. 8.

Note that for the perturbed case, the ensemble spread remains small even 2 years after the initialization, as the termination of strong El Niño events occurs in a rather predictable manner (e.g. Lengaigne et al. 2006). In contrast, the control experiment shows a very large spread after the 2 years, which indicates that the termination of a CP El Niño and the subsequent evolution of the system has little predictability.

It is noteworthy that, with the imposed WWB, the system evolution for the recharged set (Fig. 9d,e) resembles that of the observed 1997–1998 El Niño event (Fig. 1a, b). One can identify several similarities. (1) The first WWB is followed by a succession of subsequent westerly wind anomalies. (2) The initial warming generated by the first WWB has two components, one in the western-central Pacific induced by local effects and the other in the eastern Pacific induced by remote effects. (3) The EP El Niño reaches its mature phase in the wintertime of the year, with the maximum SST anomaly as large as 5 °C. (4) Before the termination of El Niño there occurs a secondary SST maximum and the entire event lasts roughly 1½ years.

3.2 Experiments results: Set 2 (neutral)

Unlike Set 1, Set 2 does not develop strong temperature or wind anomalies. Nevertheless, the system evolution in this case is still quite instructive. Specifically, without the WWB, the coupled system develops a weak La Niña. In the ensemble mean sense, the Niño3 index decreases from 0 °C to −1 °C (Fig. 5a), while the Niño4 index decreases from 1 to 0 °C by the end of the first year (Fig. 5b). This cooling in the central and eastern Pacific, which lasts about

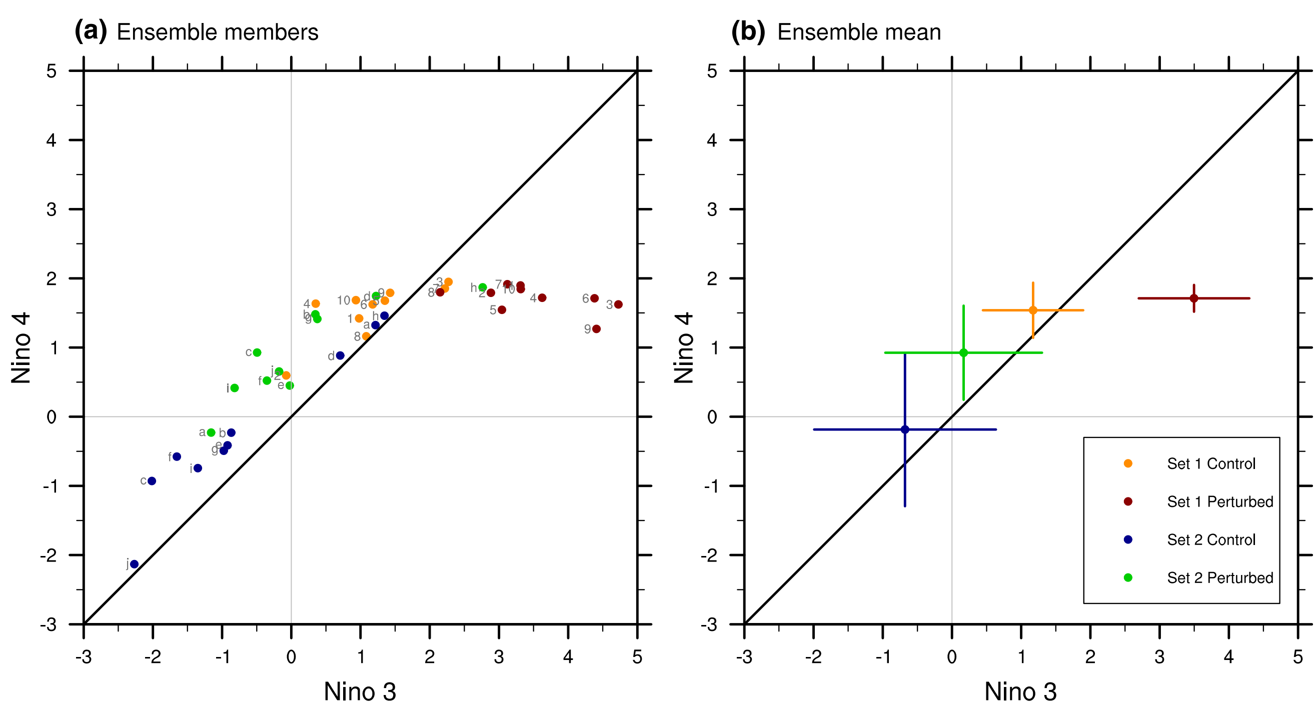

Fig. 8 Diagrams showing the Niño4 index versus the Niño3 index (in °C) at the end of the first year for (**a**) ensemble members, and (**b**) ensemble means with *bars* indicating one standard deviation. The Niño indices are averaged from October through December

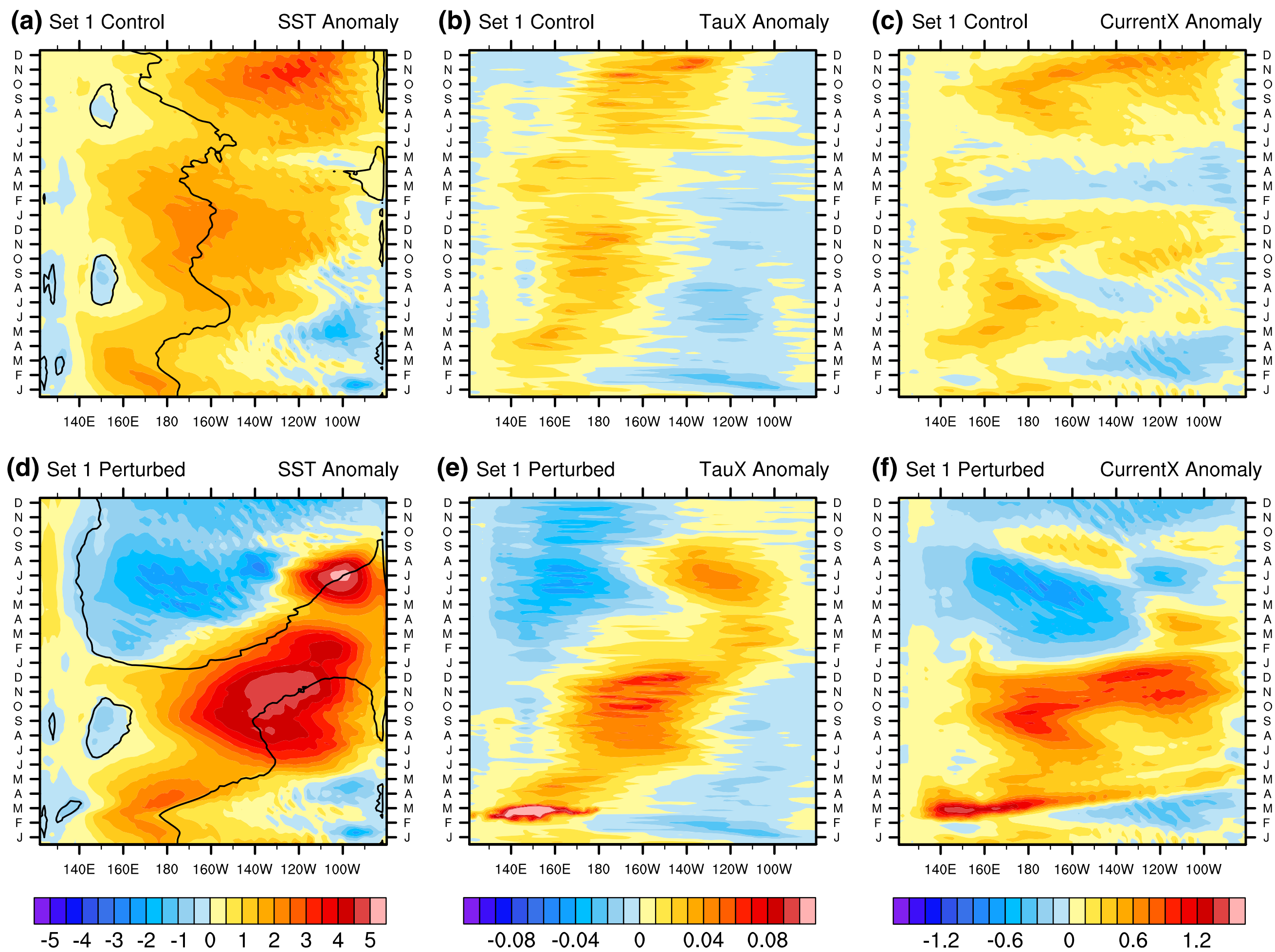

Fig. 9 Hovmoller diagrams for anomalies in (**a**, **d**) SST, (**b**, **e**) zonal wind stress and (**c**, **f**) surface zonal current for Set 1 (ensemble mean values). The *upper* (*lower*) *three panels* are for the control (perturbed) runs without (with) the imposed WWB. The corresponding contour intervals are 0.5 °C, 0.01 N/m^2, and 0.15 m/s. The *solid line* shows the 29 °C isotherm of full SST, which marks the warm pool eastern edge. All variables are averaged within the equatorial band (2°S–2°N). The time (vertical) axis goes upward. Note that the signal associated with wind-generated Kelvin waves propagates to the eastern Pacific faster than the more gradual eastward propagation of SST anomalies

1 year and indicates the occurrence of La Niña conditions, is also clearly evident in the SST spatial patterns (Fig. 7b, d) and Hovmoller diagrams (Fig. 10a).

In contrast to Set 1, the ensemble members now show a large divergence at the end of the first year, ranging from slight warming as large as 2 °C to strong cooling with the magnitude of −3 °C (Fig. 7b), although the ensemble mean still indicate a cooling event. At the peak of La Niña, differences between the end members of the ensemble for either Niño index can be as large as 5 °C (Fig. 5a, b), leading to a large standard deviation in the ensemble (Fig. 8b).

The development of La Niña conditions in this set can be also seen in the Hovmoller diagrams (Fig. 10a–c). During February–March, the whole equatorial basin is close to a neutral state (Fig. 5c), but with slightly warmer western Pacific and slightly cooler eastern Pacific relative to the climatology (Fig. 10a). The further cooling of the eastern equatorial Pacific corresponds to the strengthening of anomalous easterly winds in the central and eastern part of the basin (Fig. 10b), which intensifies upwelling in the cold tongue region and keeps warmer waters in the western Pacific. The weak La Niña conditions are followed by an El Niño event at the end of the second year (Fig. 10a).

When the WWB is imposed, Set 2 slides into a weak CP El Niño instead of the La Niña. For the ensemble mean, Niño3 index stays around zero during the first year (Fig. 5d), while the variations of Niño4 index show a small bulge near the end of the first year (Fig. 5e) of about 1 °C. While the amplitude of this event (in the ensemble mean sense) is weak, the spatial structure of the SST anomaly corresponds to a CP El Niño. Its maximum SST anomaly is

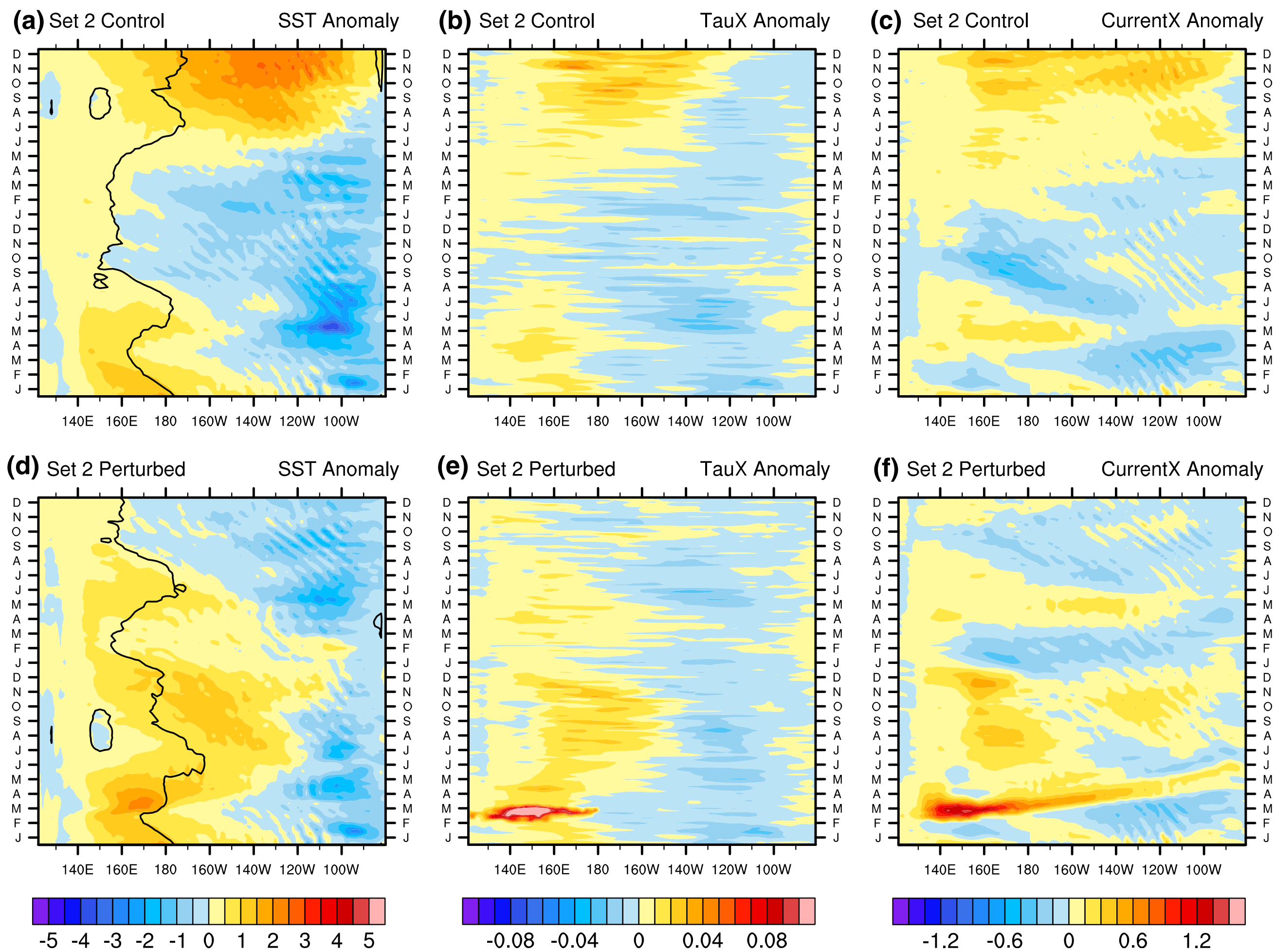

Fig. 10 As in Fig. 9 but for Set 2

centered around 160°W–170°W, and there is a slight cooling in the far eastern Pacific (Fig. 7f, h).

There is still a large divergence between different ensemble members (Figs. 5d–f, 7f, 8). Five out of ten cases develops into El Niño events (four CP events and one EP event), and one case develops into a La Niña event, while the rest fall in between (Fig. 8a). In contrast to Set 1, the perturbed experiments in Set 2 show much smaller variations in OHC, with a weak heat recharge followed by a weak discharge (Fig. 5f).

The evolution patterns of the anomalous SST, zonal wind stress, and surface zonal current show that the development of this CP El Niño event involves both local and remote effects induced by the imposed WWB, as well as subsequent ocean–atmosphere interactions. Locally, the imposed WWB pushes the warm pool eastward, and induces a warm SST anomaly as large as 2 °C in the western Pacific, which then propagates to the central Pacific (Fig. 10d). This warming however is unable to spread into the eastern equatorial Pacific, which remains colder than the climatology. Consequently, easterly surface winds persist in the eastern part of the basin.

After the CP El Niño reaches its peak, the seasonal strengthening of surface winds and the currents (not shown) pushes back the warm pool and the warm event decays, followed by a weak La Niña in the late months of the second year. This termination of the warm event resembles the “abrupt decaying pattern” discussed by Yu and Kim (2010).

3.3 Similarities between Set 1 Control and Set 2 Perturbed

A comparison between the sets immediately suggests that there are important similarities between Set 1 Control and Set 2 Perturbed, which both have CP El Niño events. This is evident both in the time evolution of the events during the first year (Figs. 9, 10, 11) and the spatial structure of warm anomalies by the end of this year (Figs. 4, 5). One reason for these similarities is that experiments in Set 1 Control actually develop their own WWBs in the beginning of the first

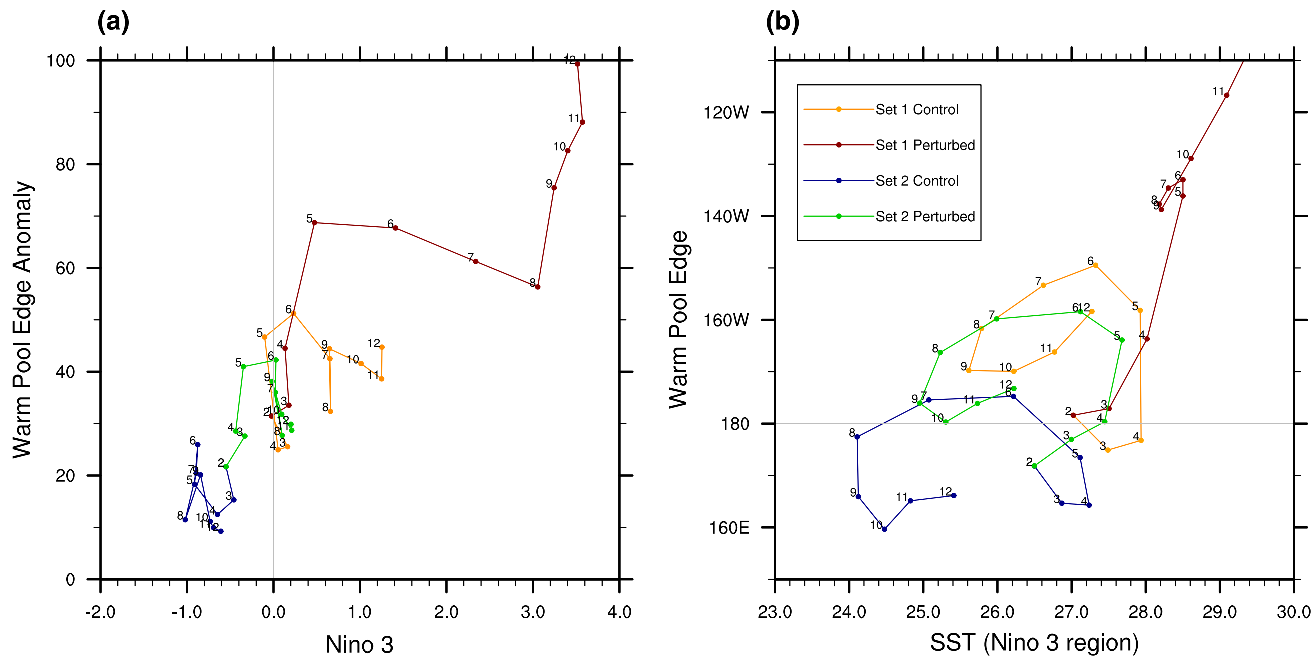

Fig. 11 Displacement of the warm pool eastern edge (in degrees of longitude) versus Niño3 SST (in °C) for different months of the year. **a** Anomalies with respect to model climatology; **b** full values with the seasonal cycle included. Both the perturbed and control experiments are shown (in the ensemble-mean sense). *Numbers* indicate months of the first year, starting from February (month 2), after which the perturbed and control experiments diverge. Note that for an EP El Niño event to develop, the warm pool should extend into the eastern Pacific, which is facilitated by WWBs

year (model-generated rather than artificially imposed), even though they are weaker than the imposed wind burst in the perturbed experiments. A signature of the model-generated WWBs is seen in the ensemble-mean Hovmoller diagram between February and May of the first year (Fig. 9b).

However, there are also some differences between the two sets. For example, in Set 2 Perturbed, the eastern Pacific is colder, so that any developing westerly wind anomalies are weaker and more confined in the western Pacific, resulting in a weaker CP event than in Set 1 Control (Figs. 9a–c, 10d–f). As mentioned already, the evolution of the CP event during the second year differs in these two sets as well (Figs. 9, 10).

Overall, the evolution and spatial structure of the events in these two sets resemble that of the El Niño events of 2002 and 2004 (Fig. 1c–f). In both cases the observed warm events were preceded by an enhanced WWB activity (perhaps not as strong as prior to the 1997-1998 El Niño), had a maximum warming in the central Pacific, and never reached too strong amplitudes.

4 Comparing the sets: how events of different types develop

To understand why the coupled system responds to the WWBs in rather different ways, we will now compare Sets 1 and 2 from several perspectives, including the initial conditions, evolution patterns, mature phases of the events, and the divergent behavior of the ensemble members.

A key characteristic of the initial ocean states most relevant for our consideration is the different OHC in the two sets at the time when WWB is imposed. The higher OHC in Set 1 (recharged state) is associated with warmer waters in the western/central equatorial Pacific. The latter factor is related to weaker easterly winds and hence weaker surface westwards currents in Set 1 (Fig. 6e, f), allowing for this set a greater eastward extension of the warm pool along the equator (by about 10° of longitude) and a slightly warmer cold tongue (by 1 °C) during the early months of the first year (Fig. 6a–d).

The different initial states result in different evolution patterns for the events. Even though ensemble members exhibit somewhat divergent behavior, in the ensemble mean sense several key differences for the two sets emerge as evident from the Hovmoller diagrams (Figs. 9, 10) and summary plots showing the month-by-month progression of two critical variables – the Niño3 SST and the position of the eastern edge of the warm pool (Fig. 11). These variables reflect changes in two different regions (the central and eastern Pacific), whose magnitude, extent and interaction control whether a CP or EP event develops.

In both sets the initial location of the eastern edge of the warm pool, defined here as the 29° isotherm, is shifted eastward as compared to the model climatology (by approximately 30° in Set 1 and 20° in Set 2, see Fig. 11a). Following the seasonal cycle, the warm pool edge moves farther east during the first half of the year (Fig. 11b). However, because of the effect of WWBs (imposed or model-generated as in Set 1 control, see Fig. 9b) and the subsequent ocean–atmosphere interactions in the western/central Pacific, the distance that the warm pool edge travels eastward varies from one set of experiments to the next. By June the warm pool edge in the different sets has shifted by about 10°, 30°, 30° or 50° of longitude farther east with respect to its initial location in February (Fig. 11b). The largest shift occurs for Set 1 Perturbed and the smallest—for Set 2 Control.

The differences in the initial position and the distance that the warm pool edge travels imply that the extent of the warm pool in the mid-year varies greatly across the sets (Figs. 9a, d, 10a, d and 11b). Whereas in Set 2 Control the warm pool edge remains in a close proximity to the dateline, in Set 1 Perturbed it reaches 135°W. The warm pool spreading eastward is associated with a slow eastward propagation of warm SST anomalies coupled to wind stress and surface current anomalies (Figs. 9, 10). The large anomalous eastward shift of the warm pool in Set 1 Perturbed is due to the strong imposed WWB and the initially weaker westward surface currents (Fig. 6e), compared with Set 2 (Fig. 6f).

Now let us consider a more remote effect of the WWBs, namely the warming of the eastern Pacific induced by wind-generated Kelvin waves. These Kelvin waves can be identified via surface current anomalies for example (Figs. 9c,f and 10f). As expected, WWBs induce a thermocline deepening in the western and central Pacific, which propagates eastward as a Kelvin wave, weakens the westward surface currents, and causes a warming in the eastern equatorial Pacific, on the order of 0.5–1 °C by May–June (Figs. 9a, d, 10a, d and 11).

The further evolution of this initial warming determines whether a CP or EP El Niño develops. In the experiments of Set 1 Control and Set 2 Perturbed, even after the initial warming, SST in the eastern equatorial Pacific in May–June remains colder or close to the climatology (Figs. 9a, 10d and 11a). The subsequent strong westward retraction of the warm pool after June-July due to the seasonal cycle (Fig. 11b) prevents the potential development of the Bjerknes feedback, and the warm events in these two cases do not develop beyond a CP El Niño.

In contrast, in Set 1 Perturbed the initial warming makes the eastern Pacific already warmer than the climatology. Even when a slight retraction of the warm pool does occur (Fig. 11b), the warm pool edge remains in the eastern Pacific which allows a virtually uninterrupted Bjerknes feedback that leads to a shift of atmospheric convection towards eastern Pacific and a strong warming of the Niño3 index, which manifest an EP event.

Thus, the location of the warm pool edge during the mid-year, when the initial warming due to the Kelvin wave occurs, turns out to be critical for the development of the events. Apparently, only conditions in which the warm pool edge has already reached the eastern equatorial Pacific by this time allows for the strong Bjerknes feedback leading to the strong warming in the east. Otherwise, the warming in the central Pacific and the initial warming in the east remain disconnected, which prevents the development of the Bjerknes feedback and allows only CP events. These findings are confirmed by the strong dependence of the Niño3 index at the end of the year on the position of the warm pool edge during the mid-year transition (Fig. 12).

Finally, looking at the ensemble members, we find that the evolution of the neutral set is much more uncertain than the recharged set. No matter whether we impose WWBs or not, the range of behavior of the ensemble members in Set 2 is much broader (Fig. 8a), and the standard deviation is much larger than that in Set 1 (Fig. 8b). Additionally, if we look at the zonal structures of the SST anomaly in the equatorial band at the peak of the events, all the ensemble members in Set 1 develop into EP El Niño events (Fig. 7e), while only five out of ten cases in Set 2 develop into clear El Niño events (four CP events and one EP event) and the rest show either no significant anomalies or anomalies consistent with La Niña (Fig. 7f). These differences are also evident in the extent of divergence of the various Niño indices (Figs. 4, 5).

5 Similarity of CP and EP events and importance of the thermocline feedback

It is well accepted that a key dynamical factor for El Niño is the thermocline feedback. In this feedback, SSTs over the eastern-central equatorial Pacific are modified by mean upwelling of subsurface temperature anomalies associated by thermocline depth anomalies (induced by wind stress anomalies). Some authors confirm the importance of thermocline variations for the development of CP events (e.g. Ashok et al. (2007), but other studies disagree and emphasize local air-sea interactions (Kao and Yu 2009) and the zonal-advection feedback (Kug et al. 2009). As we show next, our modeling results clearly point to the importance of the thermocline feedback for both types of events.

As evident from changes in the ocean thermal structure along the equator, significant thermocline displacement occurs at the peak of both types of events. It is true however that the magnitude of subsurface temperature

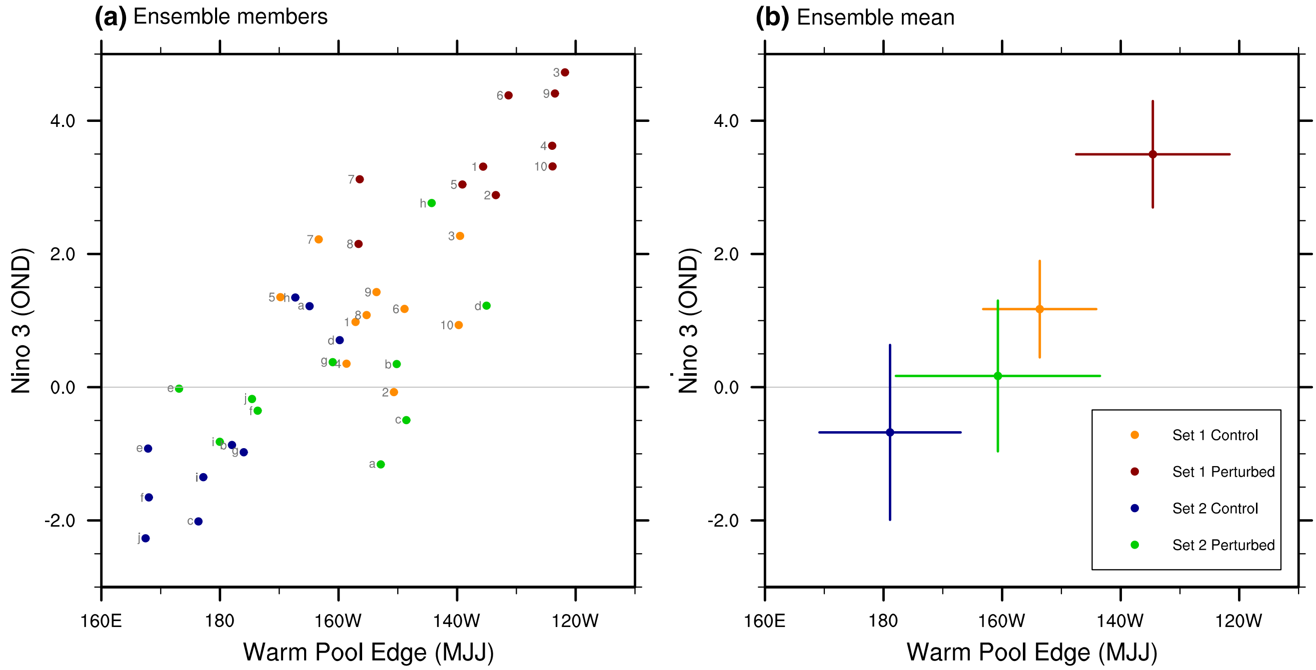

Fig. 12 The Niño3 index (in °C) by the end of the first year versus the mid-year position of the warm pool eastern edge. **a** Ensemble members; **b** ensemble means with the *bars* indicating one SD. Note the high degree of correlation between the mid-year extent of the warm pool and the subsequent Niño3 index. OND = October, November, December; MJJ = May, June, July

anomalies is on average 2–3 times smaller for CP El Niño (Fig. 13b,d), which reflects the fact that such events are generally weaker than EP El Niño events. Also, the maximum of subsurface temperature anomalies for CP events is located closer to the central Pacific and is accompanied by a negative anomaly in the very east of the basin related to persistent easterly winds in this case. As a result of these differences, the thermocline flattens in the whole equatorial basin for EP events (Fig. 13a), but only in the western and central Pacific for CP events (Fig. 13c).

To investigate the contributions of the thermocline feedback to the development of CP and EP El Niño events, we have conducted a heat budget analysis for the ocean mixed layer temperature, focusing on the role of the thermocline feedback key term ($\bar{w}\frac{\partial T'}{\partial z}$). This term, as other terms of the heat budget, was computed using monthly data, averaged over the equatorial band (2°S–2°N) and from the surface to 50 m, following the method of Kug et al. (2009). Hereafter, T is temperature; x and z—the zonal and vertical coordinates, u and w—the zonal and vertical velocity; and overbars and primes indicate the climatology and anomalies, respectively.

Figure 14 shows the Hovmoller diagrams of the thermocline feedback term for Sets 1 and 2 with and without the imposed WWBs. As expected, the thermocline feedback plays a crucial role in the development of EP Niño, and the SST warming tendency it induces can be as large as 2.5 °C/month in the eastern Pacific (Fig. 14c). The two cases associated with CP El Niño events, Set 1 Control (Fig. 14a) and Set 2 Perturbed (Fig. 14d), show evolution patterns for this term very similar to each other and, furthermore, qualitatively similar to the evolution in the EP El Niño, especially from the initial to mature stages of El Niño. The SST tendency due to the thermocline feedback for the CP events is apparently weaker than that for the EP events, but may still reach nearly 1 °C/month, dominating other terms of the heat budget (only the $u'\frac{\partial \bar{T}}{\partial x}$ term is shown in Fig. 15).

Notable difference is the variations of the key term ($\bar{w}\frac{\partial T'}{\partial z}$) are more apparent for the event termination. For EP events the strong Bjerknes feedback continues to operate throughout the entire oscillation cycle, but changes its sign, which enables a strong La Niña (Figs. 14c, 9d). For CP events however, the change in the sign of this term is brief and lasts only 2–3 months in the eastern Pacific—not a sufficient time to facilitate La Niña development. The transition between the warm and cold phases is related to the southward shift of the winds in winter generating an upwelling Kelvin wave that reverses the sign of $\frac{\partial T'}{\partial z}$ as discussed in Lengaigne et al. (2006). This wind shift is weaker for moderate events.

Here, for comparison, we also show the zonal advective feedback term $u'\frac{\partial \bar{T}}{\partial x}$, see Fig. 15. For EP El Niño, zonal

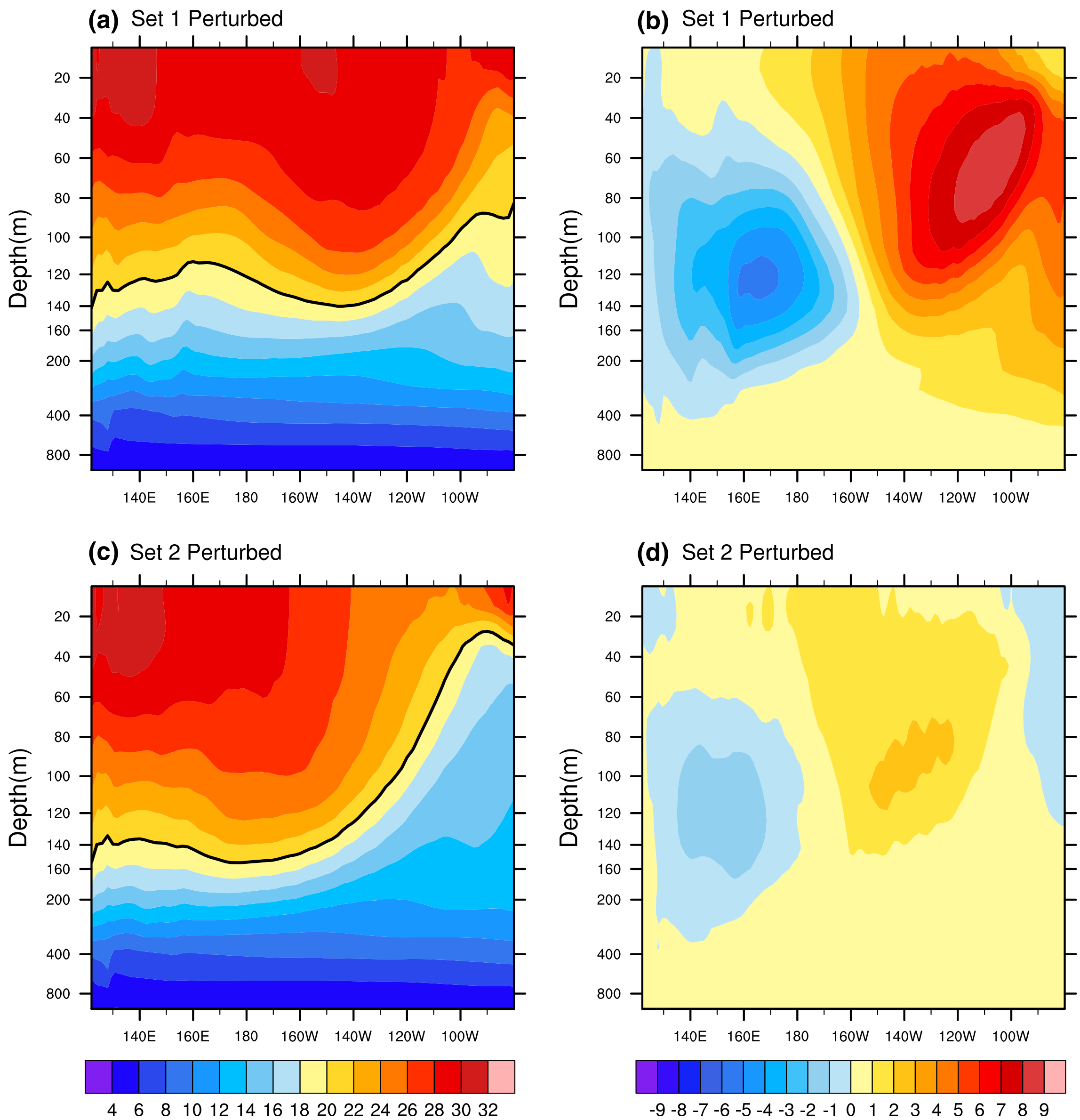

Fig. 13 Ocean thermal structures along the equator (averaged between 2°S and 2°N) at the peak of warm events in November for (**a**, **b**) Set 1 Perturbed and (**c**, **d**) Set 2 Perturbed. *Left panels* show full temperature (in °C) with the contour interval of 2 °C. *Right panels* show temperature anomalies (in °C) relative to the climatology with the contour interval of 1 °C. The *solid black line* indicates the thermocline, defined as the 20 °C isotherm. Note the nearly flat thermocline in Set 1 and both similarities and differences in the structure of temperature anomalies across the two sets

advective feedback is obviously important with the warming tendency of 1.5 °C/month (Fig. 15c). But in this and only in this case nonlinear terms become also important. In particular the nonlinear term $u' \frac{\partial T'}{\partial x}$ becomes so strong (not shown) that it offsets significantly the contribution of the zonal advective feedback. For CP El Niño events, the warming associated with the zonal advective feedback is always below 0.5 °C/month and even negative in central-eastern Pacific from June to August; consequently its contribution to the development of warm events is rather limited compared with the thermocline feedback (Fig. 15a, d). Note that in Set 2 Control, the cooling effects induced by the zonal advective feedback appear to be associated with the development of the weak La Niña (Fig. 15b).

Other advection terms (not shown here) can also contribute to the development of EP and CP El Nino, even though their magnitudes are smaller than the two aforementioned feedbacks (thermocline and zonal advection). For instance, in Set 1 Perturbed, the Ekman feedback term $w' \frac{\partial \bar{T}}{\partial x}$ is also important for the development of EP El Niño, especially in the eastern Pacific.

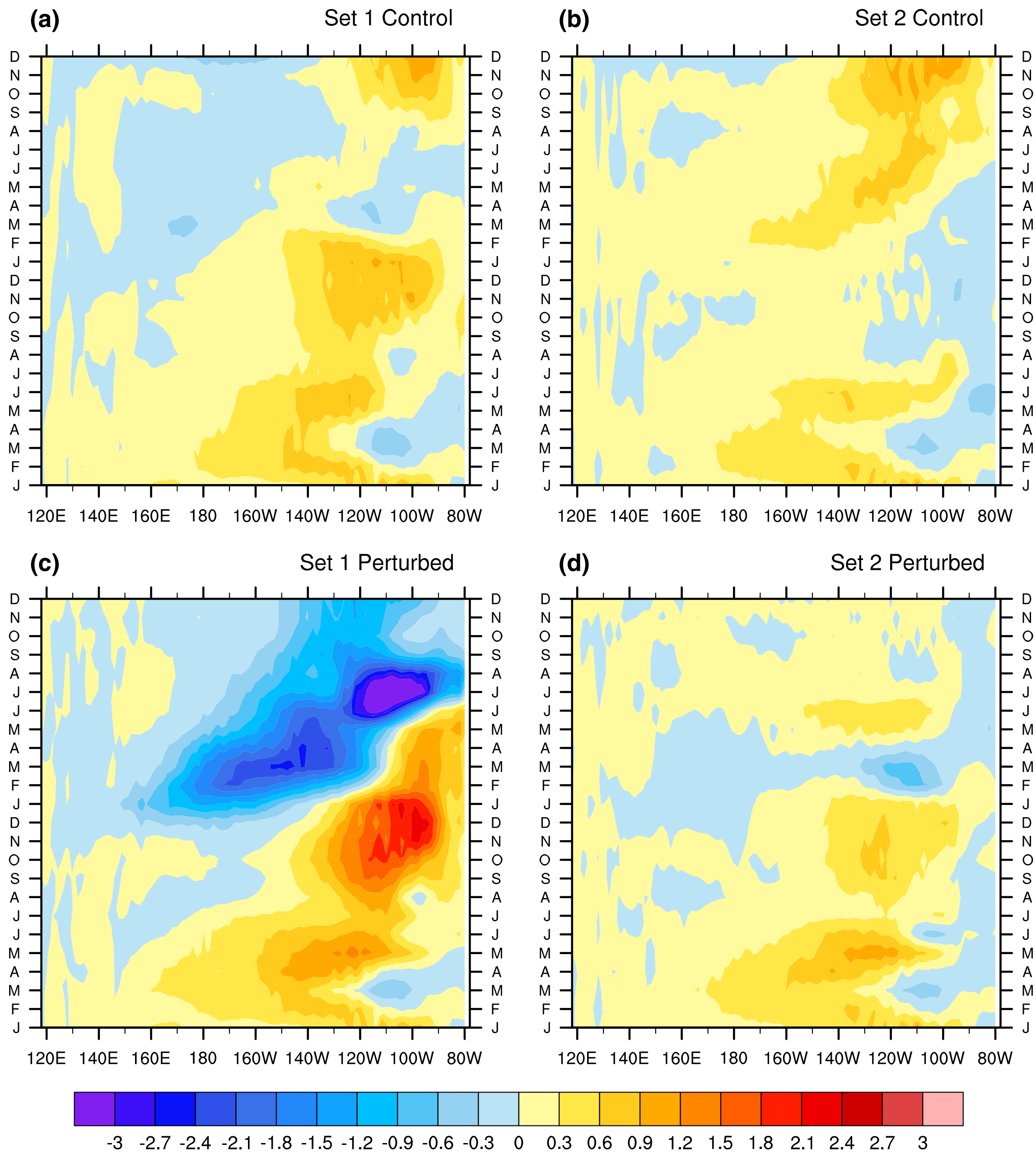

Fig. 14 Hovmoller diagrams for the ensemble mean of the thermocline feedback term (in °C/month) for (**a**) Set 1 Control, (**b**) Set 2 Control, (**c**) Set 1 Perturbed, and (**d**) Set 2 Perturbed. Contour interval is 0.3 °C/month

6 How different the two El Niño flavors are: implications for extreme events

As shown in the previous section, the two types of El Niño share the importance of thermocline feedback in our model, even though the magnitude of thermocline anomalies and the overall strength of this feedback are greater for EP events. This raises the question of how different the two types of events really are. In other words, do they belong to two discrete classes of El Niño or simply to a broad continuum of events? It turns out that the answer to this question depends on how we approach the question, or more exactly which metric we use to compare the events.

For example, one could define the type of El Niño according to where (which longitude) the maximum SST anomaly occurs at the peak of warm events. According to this definition, we obtain two clearly defined groups of events with the SST maximum located east or west of 150°W (the boundary between the Niño3 and Niño4

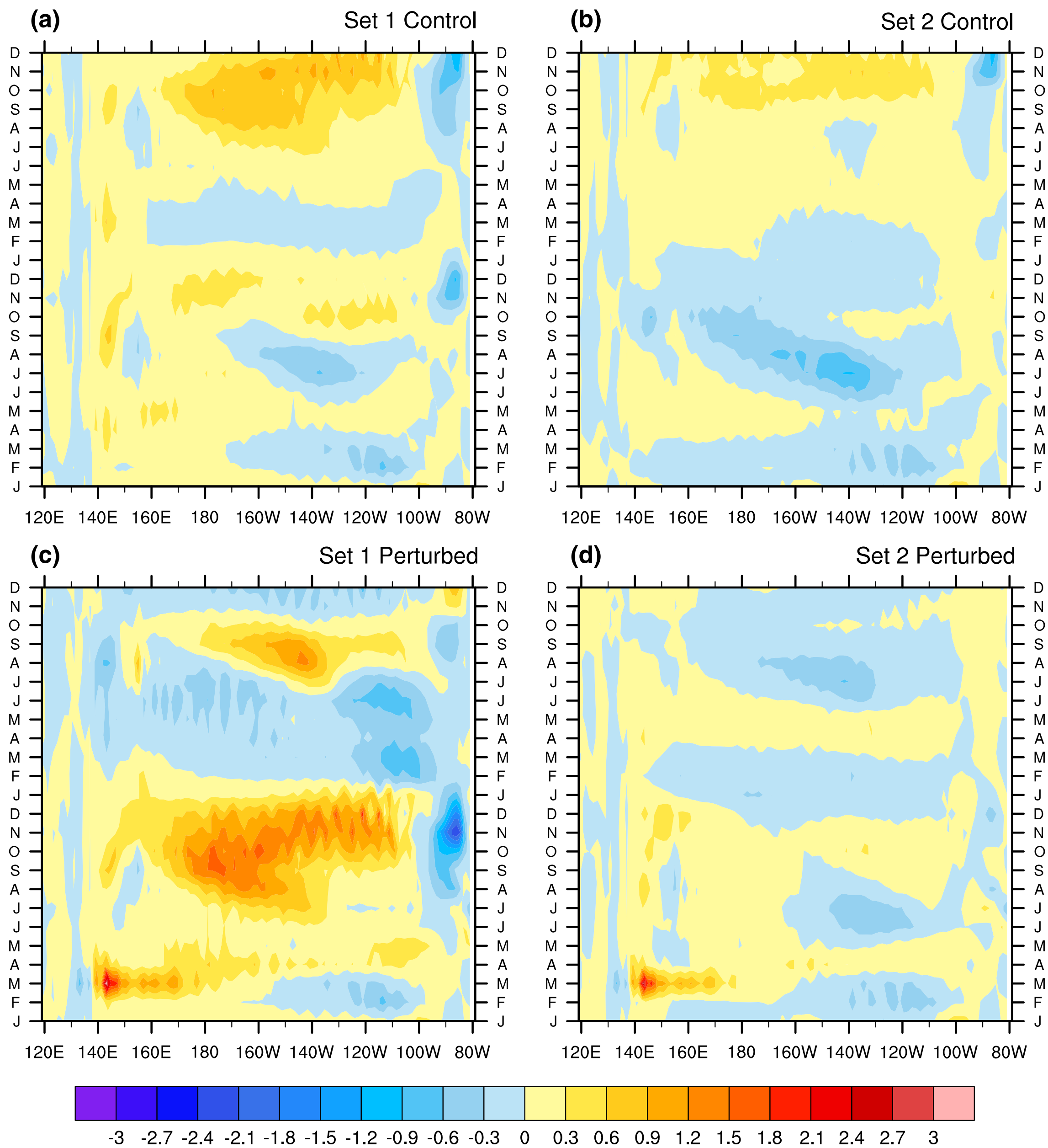

Fig. 15 As in Fig. 14 but for ensemble mean of the zonal-advection feedback term

boxes), see Fig. 16a. From this viewpoint, CP and EP events seem to belong to two discrete types of El Niño.

Alternatively, one could assess the events using the magnitude of the SST anomaly averaged over the central and eastern equatorial Pacific between 2°S–2°N and 160°E–90°W, which combines the Niño3 and Niño4 regions, and the average location of the SST anomaly (as done in Giese and Ray 2011, for example). The latter parameter is given by the location of the anomaly heat center defined as

$$\text{Heat center} = \frac{\int SSTA(x) \cdot x \cdot dx}{\int SSTA(x) \cdot dx},$$

where integration is conducted with respect to longitude within the equatorial band in the Pacific, and SSTA stands for SST anomaly.

This latter, averaging approach reveals that the warm events in the model actually fall on one line, and stronger events are associated with a more easterly location of the heat center (Fig. 16b). There is no critical longitude

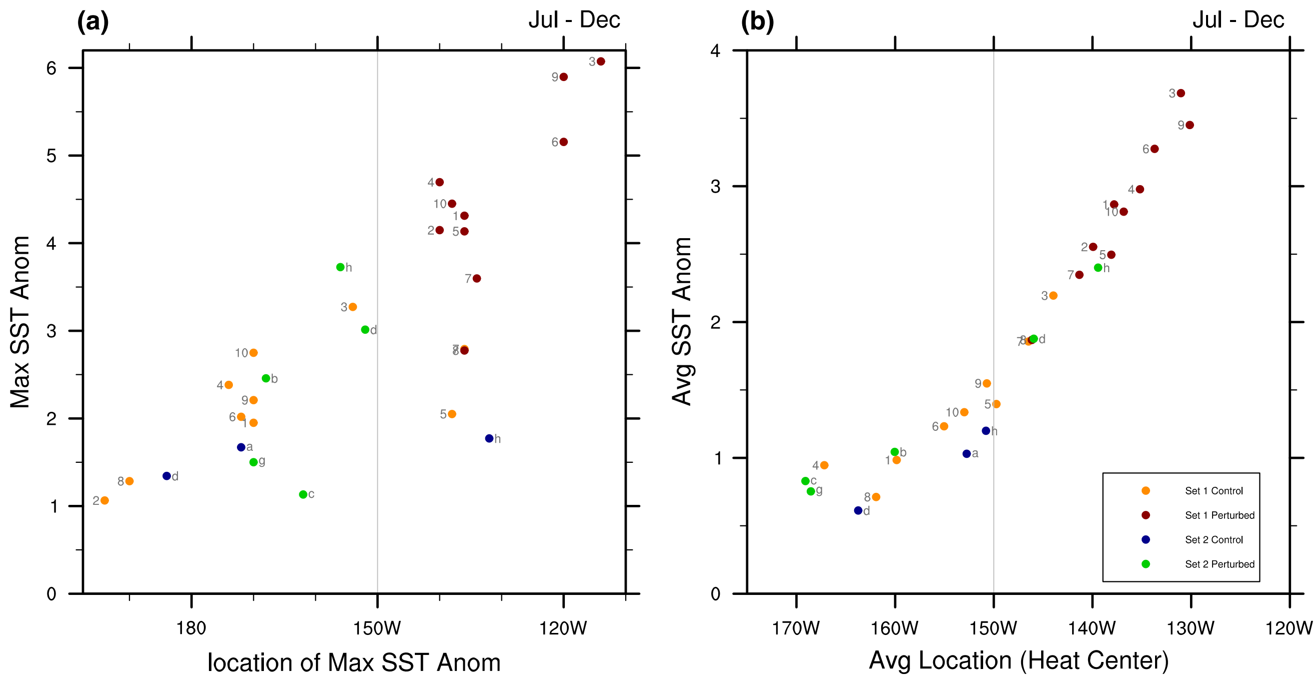

Fig. 16 **a** The maximum of the SST anomaly (in °C) within the Niño4-Niño3 region versus its exact location along the equator. **b** Average SST anomaly (in °C) within the Niño4–Niño3 region versus the average location of this anomaly given by the heat center. Each dot indicates a warm event from our simulations. All warm events from Sets 1 and 2, with and without the imposed WWB, have been included. Anomalies are averaged from July to December and computed with respect to the model climatology. Note that Case 2 of Set 1 Control was not included in the *right panel* because its average SST anomaly is close to zero (Fig. 7a). For the definition of the heat center see the text

separating the two groups, which now appear as a continuum with a linear relationship between the warming amplitude and the heat center location (Fig. 16b). Hence, in this sense, CP and EP El Niño events should not be viewed as totally different types. This reflects the fact that many of the events we observe are of the mixed nature (scattered in the vicinity of the diagonal line in the diagram of Fig. 8a).

Differences between EP El Niño and CP El Niño do manifest strongly in the occurrence of extreme warm events. As it is clear from Fig. 16, only EP events are able to reach strong amplitudes. Moreover, as seen from the Niño indices, among the forty experiments in our study only three events develop into extreme EP El Niño with Niño3 index exceeding 4.5 °C (Fig. 8a), and they all result from a combination of a strong preceding WWB and the recharged initial ocean state. The maximum SST change observed in these experiments reaches about 6 °C (Fig. 7e) and reminds the temperature anomaly observed in 1997/1998.

Even given favorable conditions, the development of extreme El Niño events involves large uncertainty. For example, without the imposed WWBs, experiments 5 and 9 in Set 1 would develop into CP El Niño events with almost the same amplitudes (Fig. 8a). Nevertheless, after we imposed the WWB, experiment 5 slides into a moderate event, while experiment 9 develops an extreme EP El Nino (Fig. 8a). The large uncertainty involved in the generation of extreme events is further highlighted by the fact that the amplitude of two extreme events exceeds one standard deviation of the ensemble (Figs. 4d, 7e). Thus, the occurrence of extreme events can result (but not always) from a combination of strong WWB activity and appropriate initial conditions of the coupled system.

7 Conclusions

In this study, using a suite of simulations with a comprehensive coupled model, we show how the effect of westerly wind bursts can lead to the development of different El Niño characteristics (with Central Pacific or Eastern Pacific warming). The particular response of the system to these wind perturbations is determined by the initial state of the ocean, the strength of the wind burst, and the subsequent ocean–atmosphere interactions. We find that a heat recharge state can develop into either a CP El Niño (after a weak wind burst) or EP El Niño (after a stronger burst). A neutral state typically develops into a CP event after a strong burst.

An important factor in the developments of warm events is the interplay between the eastward shift of the warm pool (initiated by a surface current relaxation associated with the wind burst) and the warming of the eastern equatorial Pacific (initiated by the wind-induced Kelvin waves), both facilitated by ocean–atmosphere coupling. How far the eastern edge of the warm pool extends by the time that the initial warming in the eastern Pacific occurs appears to be critical to which type of El Niño can develop. In our model, only if the warm pool edge has already entered the eastern Pacific by the time that the warming due to Kelvin waves begins, can there develop an EP event, which is driven by an uninterrupted Bjerknes feedback that couples SST, thermocline and the winds over the entire equatorial basin. However, if the initial warmings in the central Pacific and eastern Pacific remain disconnected and the subsequent warming of the eastern Pacific is accompanied by the retreat of the warm pool edge, the Bjerknes feedback is interrupted and only a CP event ensues (Fig. 11).

In contrast to some previous studies, we show that the event development is strongly influenced by the thermocline feedback for both types of El Niño, not just EP events. Even though in the CP case thermocline variations are weaker and their strongest impact is shifted more towards the central Pacific, the thermocline feedback term gives an important contribution to the positive SST tendency in the central Pacific (Fig. 14). An ocean energetics perspective (Hu et al. 2014) also supports the importance of thermocline variations for CP events.

Here, it is important to note the connection of the different types of events to the seasonal cycle in the tropical basin. As apparent from Fig. 11b, the CP El Niño could be viewed as a modulation (weaker or stronger) of the seasonal cycle, which involves ocean–atmosphere coupling. While the EP El Niño does begin as a modulation of the seasonal cycle, in the second half of the year, when the Bjerknes feedback is amplifying, its development qualitatively and quantitatively diverges from the latter. The relationship between different flavors of El Niño and the annual cycle will be further discussed elsewhere.

Looking at the individual members of the ensemble experiments, we also find several important results. In particular, the predictability of El Niño and La Niña events when the ocean is initially at a neutral state is inherently limited. With or without WWBs, the ensemble members in the neutral set show a much more divergent behavior as compared with those in the recharged set. In fact, while most of the ensemble members in the perturbed neutral set develop a CP El Niño, one experiment slides into a weak La Nina, while another one evolves into an EP El Niño (Fig. 8a).

While there is more predictability in the recharged set (because of less divergence between ensemble members), the actual amplitude of the warm events would be difficult to predict (Fig. 8). There are three experiments in this set that eventually develop into extreme El Niño with the Niño3 index exceeding 4.5 °C. Two of the extreme warm events lie beyond one standard deviation from the ensemble mean (Figs. 4d, 7e). However, even slight differences in the initial conditions can change the situation, leading to the development of weaker events. Thus, the occurrence of extreme El Niño events results from a combination of strong WWB activity and the appropriate state of the coupled system, and involves further uncertainty associated with chaotic atmospheric dynamics.

Our results suggest that the CP and EP El Niño could be viewed as end members of one continuum (in a general agreement with the conclusions of Giese and Ray 2011) rather than two discrete classes of El Niño. These different views depend on whether one focuses on the maximum SST anomaly and the exact longitude where it occurs, or on the averaged warming magnitude and the anomaly heat center. In the latter view, our model results show that there is a smooth transition between El Niño "flavors", and that the warming amplitude is almost linearly related to the location of the heat center for all El Niño events (Fig. 16b). That is, the more eastward the heat center is located, the stronger averaged warming magnitude is. This is because in the eastern Pacific, SST is generally colder, which makes it easier to generate large positive temperature anomalies than in the central Pacific. Thus, these two views give complementary perspectives on the diversity of El Niño events.

Acknowledgments This research was supported by Grants from NSF (AGS-1116885), DOE Office of Science (DE-SC0007037), the David and Lucile Packard Foundation, and the Agence Nationale de la Recherche (ANR) project METRO (2010-BLAN-616-01).

References

An SI, Jin FF (2001) Collective role of thermocline and zonal advective feedbacks in the ENSO mode. J Clim 14(16):3421–3432. doi:10.1175/1520-0442(2001)014<3421:Crotaz>2.0.Co;2

Ashok K, Behera SK, Rao SA, Weng HY, Yamagata T (2007) El Nino Modoki and its possible teleconnection. J Geophys Res-Oceans 112(C11). doi:10.1029/2006jc003798

Battisti DS, Hirst AC (1989) Interannual variability in a tropical atmosphere ocean model—influence of the basic state, ocean geometry and nonlinearity. J Atmos Sci 46(12):1687–1712. doi:10.1175/1520-0469(1989)046<1687:Iviata>2.0.Co;2

Boulanger JP, Menkes C (1999) Long equatorial wave reflection in the Pacific Ocean from TOPEX/POSEIDON data during the 1992–1998 period. Clim Dyn 15(3):205–225. doi:10.1007/S003820050277

Boulanger JP, Menkes C, Lengaigne M (2004) Role of high-and low-frequency winds and wave reflection in the onset, growth and termination of the 1997–1998 El Nino. Clim Dyn 22(2–3):267–280

Clarke AJ (2008) An introduction to the dynamics of El Nino & the southern oscillation. Academic Press, London

Clarke AJ (2010) Analytical theory for the quasi-steady and low-frequency equatorial ocean response to wind forcing: the "Tilt" and "Warm Water Volume" modes. J Phys Oceanogr 40(1):121–137. doi:10.1175/2009jpo4263.1

Ding QH, Steig EJ, Battisti DS, Kuttel M (2011) Winter warming in West Antarctica caused by central tropical Pacific warming. Nat Geosci 4(6):398–403. doi:10.1038/Ngeo1129

Drushka K, Bellenger H, Guilyardi E, Lengaigne M, Vialard J, Madec G (2014) Processes driving intraseasonal displacements of the eastern edge of the warm pool: the contribution of westerly wind events. Clim Dyn (submitted)

Eisenman I, Yu LS, Tziperman E (2005) Westerly wind bursts: ENSO's tail rather than the dog? J Clim 18(24):5224–5238. doi:10.1175/Jcli3588.1

Fedorov AV (2002) The response of the coupled tropical ocean-atmosphere to westerly wind bursts. Q J R Meteor Soc 128(579): 1–23

Fedorov AV (2010) Ocean response to wind variations, warm water volume, and simple models of ENSO in the low-frequency approximation. J Clim 23(14):3855–3873. doi:10.1175/2010jcli3044.1

Fedorov AV, Philander SG (2000) Is El Nino changing? Science 288(5473):1997–2002. doi:10.1126/Science.288.5473.1997

Fedorov AV, Philander SG (2001) A stability analysis of tropical ocean-atmosphere interactions: bridging measurements and theory for El Nino. J Clim 14(14):3086–3101. doi:10.1175/1520-0442(2001)014<3086:Asaoto>2.0.Co;2

Fedorov AV, Harper SL, Philander SG, Winter B, Wittenberg A (2003) How predictable is El Nino? B Am Meteorol Soc 84(7):911. doi:10.1175/Bams-84-7-911

Gebbie G, Eisenman I, Wittenberg A, Tziperman E (2007) Modulation of westerly wind bursts by sea surface temperature: a semistochastic feedback for ENSO. J Atmos Sci 64(9): 3281–3295

Gierach MM, Lee T, Turk D, McPhaden MJ (2012) Biological response to the 1997–98 and 2009–10 El Nino events in the equatorial Pacific Ocean. Geophys Res Lett 39. doi:10.1029/2012gl051103

Giese BS, Ray S (2011) El Niño variability in simple ocean data assimilation (SODA), 1871–2008. J Geophys Res-Oceans 116(C2). doi:10.1029/2010JC006695

Guilyardi E (2006) El Niño–mean state–seasonal cycle interactions in a multi-model ensemble. Clim Dyn 26(4):329–348

Hu S, Fedorov AV, Lengaigne M, Guilyardi E (2014) The impact of westerly wind bursts on the diversity, and predictability of El Niño events: an ocean energetics perspective. Geophys Res Lett (in revision)

Hu ZZ, Kumar A, Jha B, Wang WQ, Huang BH, Huang BY (2012) An analysis of warm pool and cold tongue El Nios: air-sea coupling processes, global influences, and recent trends. Clim Dyn 38(9–10):2017–2035. doi:10.1007/S00382-011-1224-9

Jin FF (1997a) An equatorial ocean recharge paradigm for ENSO.1. Conceptual model. J Atmos Sci 54(7):811–829. doi:10.1175/1520-0469(1997)054<0811:Aeorpf>2.0.Co;2

Jin FF (1997b) An equatorial ocean recharge paradigm for ENSO.2. A stripped-down coupled model. J Atmos Sci 54(7):830–847. doi:10.1175/1520-0469(1997)054<0830:Aeorpf>2.0.Co;2

Jin FF, Neelin JD (1993a) Modes of interannual tropical ocean–atmosphere Interaction—a unified view. 1. Numerical results. J Atmos Sci 50(21):3477–3503. doi:10.1175/1520-0469(1993)050<3477:Moitoi>2.0.Co;2

Jin FF, Neelin JD (1993b) Modes of interannual tropical ocean–atmosphere interaction—a unified view. 3. Analytical results in fully coupled cases. J Atmos Sci 50(21):3523–3540. doi:10.1175/1520-0469(1993)050<3523:Moitoi>2.0.Co;2

Kao HY, Yu JY (2009) Contrasting eastern-Pacific and central-Pacific types of ENSO. J Clim 22(3):615–632. doi:10.1175/2008jcli2309.1

Kessler WS (2002) Is ENSO a cycle or a series of events? Geophys Res Lett 29(23). doi:10.1029/2002gl015924

Kim HM, Webster PJ, Curry JA (2009) Impact of shifting patterns of Pacific Ocean warming on north Atlantic tropical cyclones. Science 325(5936):77–80. doi:10.1126/Science.1174062

Kug JS, Jin FF, An SI (2009) Two types of El Nino events: cold tongue El Nino and warm pool El Nino. J Clim 22(6): 1499–1515. doi:10.1175/2008jcli2624.1

Kumar KK, Rajagopalan B, Hoerling M, Bates G, Cane M (2006) Unraveling the mystery of Indian monsoon failure during El Nino. Science 314:115–119

L'Heureux ML, Collins DC, Hu ZZ (2013) Linear trends in sea surface temperature of the tropical Pacific Ocean and implications for the El Nino-Southern Oscillation. Clim Dyn 40(5–6):1223–1236. doi:10.1007/S00382-012-1331-2

Larkin NK, Harrison DE (2005) On the definition of El Nino and associated seasonal average US weather anomalies. Geophys Res Lett 32(13). doi:10.1029/2005gl022738

Lee T, McPhaden MJ (2010) Increasing intensity of El Nino in the central-equatorial Pacific. Geophys Res Lett 37. doi:10.1029/2010gl044007

Lengaigne M, Vecchi GA (2010) Contrasting the termination of moderate and extreme El Nino events in coupled general circulation models. Clim Dyn 35(2–3):299–313

Lengaigne M, Boulanger JP, Menkes C, Masson S, Madec G, Delecluse P (2002) Ocean response to the March 1997 Westerly Wind Event. J Geophys Res-Oceans 107(C12). doi:10.1029/2001jc000841

Lengaigne M, Boulanger JP, Menkes C, Madec G, Delecluse P, Guilyardi E, Slingo J (2003) The March 1997 Westerly Wind Event and the onset of the 1997/98 El Nino: understanding the role of the atmospheric response. J Clim 16(20):3330–3343. doi:10.1175/1520-0442(2003)016<3330:Tmwwea>2.0.Co;2

Lengaigne M, Guilyardi E, Boulanger JP, Menkes C, Delecluse P, Inness P, Cole J, Slingo J (2004) Triggering of El Nino by westerly wind events in a coupled general circulation model. Clim Dyn 23(6):601–620. doi:10.1007/S00382-004-0457-2

Lengaigne M, Boulanger JP, Menkes C, Spencer H (2006) Influence of the seasonal cycle on the termination of El Niño events in a coupled general circulation model. J Clim 19(9):1850–1868

Lian T, Chen D (2012) An evaluation of rotated EOF analysis and its application to tropical Pacific SST variability. J Clim 25(15): 5361–5373

Lopez H, Kirtman BP, Tziperman E, Gebbie G (2013) Impact of interactive westerly wind bursts on CCSM3. Dyn Atmos Oceans 59:24–51. doi:10.1016/J.Dynatmoce.2012.11.001

McPhaden MJ (1999) Genesis and evolution of the 1997–1998 El Nino. Science 283(5404):950–954. doi:10.1126/Science.283.5404.950

McPhaden MJ, Yu X (1999) Equatorial waves and the 1997–1998 El Nino. Geophys Res Lett 26(19):2961–2964. doi:10.1029/1999gl004901

McPhaden MJ, Lee T, McClurg D (2011) El Niño and its relationship to changing background conditions in the tropical Pacific Ocean. Geophys Res Lett 38(15):L15709

Neelin JD, Jin FF (1993) Modes of interannual tropical ocean–atmosphere interaction—a unified view. 2. Analytical results in the weak-coupling limit. J Atmos Sci 50(21):3504–3522. doi:10.1175/1520-0469(1993)050<3504:Moitoi>2.0.Co;2

Newman M, Shin SI, Alexander MA (2011) Natural variation in ENSO flavors. Geophys Res Lett 38(14). doi:10.1029/2011GL047658

Nicholls N (2008) Recent trends in the seasonal and temporal behaviour of the El Nino-Southern Oscillation. Geophys Res Lett 35(19). doi:10.1029/2008gl034499

Philander SG (1990) El Niño, La Niña, and the southern oscillation International geophysics series, vol 46. Academic Press, San Diego

Philander SG, Fedorov A (2003) Is El Nino sporadic or cyclic? Annu Rev Earth Pl Sc 31:579–594. doi:10.1146/Annurev.Earth.31.100901.141255

Rasmusson EM, Carpenter TH (1982) Variations in tropical sea surface temperature and surface wind fields associated with the Southern Oscillation/El Niño. Mon Weather Rev 110(5): 354–384

Sarachik ES, Cane MA (2010) The El Niño-Southern oscillation phenomenon. Cambridge University Press, Cambridge, New York

Schopf PS, Suarez MJ (1988) Vacillations in a coupled ocean atmosphere model. J Atmos Sci 45(3):549–566. doi:10.1175/1520-0469(1988)045<0549:Viacom>2.0.Co;2

Shi L, Hendon HH, Alves O, Wheeler MC, Anderson D, Wang G (2011) On the importance of initializing the stochastic part of the atmosphere for forecasting the 1997/1998 El Niño. Clim Dyn 37(1–2):313–324

Takahashi K, Montecinos A, Goubanova K, Dewitte B (2011) ENSO regimes: Reinterpreting the canonical and Modoki El Niño. Geophys Res Lett 38(10). doi:10.1029/2011GL047364

Thompson CJ, Battisti DS (2000) A linear stochastic dynamical model of ENSO. Part I: model development. J Clim 13(15): 2818–2832. doi:10.1175/1520-0442(2000)013<2818:Alsdmo>2.0.Co;2

Thompson CJ, Battisti DS (2001) A linear stochastic dynamical model of ENSO. Part II: analysis. J Clim 14(4):445–466. doi:10.1175/1520-0442(2001)014<0445:Alsdmo>2.0.Co;2

Trenberth KE, Stepaniak DP (2001) Indices of El Niño evolution. J Clim 14(8):1697–1701

Vecchi GA, Wittenberg AT, Rosati A (2006) Reassessing the role of stochastic forcing in the 1997–1998 El Niño. Geophys Res Lett 33(1). doi:10.1029/2005GL024738

Wang CZ (2001) A unified oscillator model for the El Nino-Southern Oscillation. J Clim 14(1):98–115. doi:10.1175/1520-0442(2001)014<0098:Auomft>2.0.Co;2

Wyrtki K (1975) El Nino—dynamic-response of equatorial pacific ocean to atmospheric forcing. J Phys Oceanogr 5(4):572–584. doi:10.1175/1520-0485(1975)005<0572:Entdro>2.0.Co;2

Yeh SW, Kirtman BP, Kug JS, Park W, Latif M (2011) Natural variability of the central Pacific El Nino event on multi-centennial timescales. Geophys Res Lett 38. doi:10.1029/2010gl045886

Yeh SW, Kug JS, Dewitte B, Kwon MH, Kirtman BP, Jin FF (2009) El Nino in a changing climate. Nature 461(7263):511–514. doi:10.1038/Nature08316

Yu JY, Kao HY (2007) Decadal changes of ENSO persistence barrier in SST and ocean heat content indices: 1958–2001. J Geophys Res-Atmos 112(D13). doi:10.1029/2006jd007654

Yu JY, Kim ST (2010) Three evolution patterns of Central-Pacific El Nino. Geophys Res Lett 37. doi:10.1029/2010gl042810

Yu JY, Kim ST (2011) Relationships between extratropical sea level pressure variations and the Central Pacific and Eastern Pacific types of ENSO. J Clim 24(3):708–720. doi:10.1175/2010jcli3688.1

Zubiaurre I, Calvo N (2012) The El Nino-Southern Oscillation (ENSO) Modoki signal in the stratosphere. J Geophys Res-Atmos 117. doi:10.1029/2011jd016690